particles

IMPACT FACTOR 1.7

CITESCORE 3.2

Article

General Three-Body Problem in Conformal-Euclidean Space: New Properties of a Low-Dimensional Dynamical System

Ashot S. Gevorkyan, Aleksander V. Bogdanov and Vladimir V. Mareev

Special Issue

Selected Papers from "The Modern Physics of Compact Stars and Relativistic Gravity 2023"

Edited by

Prof. Dr. Aram Saharian

MDPI

https://doi.org/10.3390/particles7040063

particles

MDPI

Article

General Three-Body Problem in Conformal-Euclidean Space: New Properties of a Low-Dimensional Dynamical System

Ashot S. Gevorkyan [1,2,*], Aleksander V. Bogdanov [3] and Vladimir V. Mareev [3]

[1] Institute for Informatics and Automation Problems, National Academy of Sciences of the Republic of Armenia, 1 P. Sevak Str., Yerevan 0014, Armenia
[2] A. B. Nalbandyan Institute of Chemical Physics, National Academy of Sciences of the Republic of Armenia, 5/2 P. Sevak Str., Yerevan 0014, Armenia
[3] Department of Fundamental Informatics and Distributed Systems, St. Petersburg State University, 7/9 Universitetskaya nab., St. Petersburg 199034, Russia; a.v.bogdanov@spbu.ru (A.V.B.); v.mareev@spbu.ru (V.V.M.)
* Correspondence: g_ashot@sci.am

Abstract: Despite the huge number of studies of the three-body problem in physics and mathematics, the study of this problem remains relevant due to both its wide practical application and taking into account its fundamental importance for the theory of dynamical systems. In addition, one often has to answer the cognitive question: is irreversibility fundamental for the description of the classical world? To answer this question, we considered a reference classical dynamical system, the general three-body problem, formulating it in conformal Euclidean space and rigorously proving its equivalence to the Newtonian three-body problem. It has been proven that a curved configuration space with a local coordinate system reveals new hidden symmetries of the internal motion of a dynamical system, which makes it possible to reduce the problem to a sixth-order system instead of the eighth order. An important consequence of the developed representation is that the chronologizing parameter of the motion of a system of bodies, which we call internal time, differs significantly from ordinary time in its properties. In particular, it more accurately describes the irreversible nature of multichannel scattering in a three-body system and other chaotic properties of a dynamical system. The paper derives an equation describing the evolution of the flow of geodesic trajectories, with the help of which the entropy of the system is constructed. New criteria for assessing the complexity of a low-dimensional dynamical system and the dimension of stochastic fractal structures arising in three-dimensional space are obtained. An effective mathematical algorithm is developed for the numerical simulation of the general three-body problem, which is traditionally a difficult-to-solve system of stiff ordinary differential equations.

Keywords: classical three-body problem; irreversibility; three-dimensional manifold; entropy of low-dimensional system; complexity; chaos; stochastic fractal; stiff ODEs system

Citation: Gevorkyan, A.S.; Bogdanov, A.V.; Mareev, V.V. General Three-Body Problem in Conformal-Euclidean Space: New Properties of a Low-Dimensional Dynamical System. *Particles* **2024**, *7*, 1038–1061. https://doi.org/10.3390/particles7040063

Academic Editor: Aram Saharian

Received: 17 September 2024
Revised: 27 October 2024
Accepted: 2 November 2024
Published: 20 November 2024

1. Introduction

The initial formulation of the three-body problem in physics and mechanics was to describe the trajectories of particles with point masses by Newton's equations of motion, taking into account the fact that particles interact according to Newton's law of universal gravitation, when the initial positions and velocities of the bodies are given [1]. Over time, it became clear that the three-body problem describes a significant number of elementary atomic-molecular processes known to us, which stimulated new research of problem taking into account the multichannel scattering of three bodies (see diagram in Figure 1) and the three-particle interaction between them [2]. It is obvious that in this case the computational complexity of the problem increases significantly for a number of well-known reasons, especially if we take into account that in many cases elementary processes are irreversible, whereas it is well known that in classical mechanics the time is reversible. Recall that this

follows from the mathematical formulation of classical mechanics, time t enters through the second-order operator $\partial^2/\partial t^2$, which means that the operator and, accordingly, the Equation are invariant under the transformation $t \to -t$. In this regard, the paper [3] pose a reasonable question to researchers, namely: is irreversibility fundamental to the description of the classical world? Note that this question turns out to play a key role in solving the problem of matching the quantum-classical transition [4,5]. In other words, new research, in addition to the goal of reducing the mathematical complexity of the problem, should answer a number of conceptual questions, and primarily the question of the irreversibility of a number of classical elementary atomic-molecular processes associated with time. Ideally, time as a measure of the movement of a dynamical system should accurately reflect the speed, nature and peculiarities of the changes occurring in the system.

Recall that time is one of the basic concepts of philosophy and physics. This is a measure of the duration and continuous existence of all material objects, a characteristic of the sequential change in their states in processes and the processes themselves, occurring in an obviously irreversible sequence from the past, through the present to the future [6–8]. However, as is rightly noted in the work [9], various physical theories, old and new, "do not fit together" with respect to some fundamental concepts and phenomena, in particular, determinism and the irreversibility of time.

$$1 + (23) \longrightarrow \begin{cases} 1 + (23), \\ 1+2+3, \\ (12) + 3, \\ (13) + 2, \\ (123)^{\star} \longrightarrow \begin{cases} 1 + (23), \\ 1+2+3, \\ (12) + 3, \\ (13) + 2, \\ (123)^{\star\star} \to \{ \ldots \end{cases} , \end{cases}$$

Figure 1. The problem of multichannel scattering in a classical three-body system can be represented in the most general form, as shown in the diagram, where 1, 2 and 3 denote interacting particles, brackets $(\cdots)$ denote a coupled system of two bodies, and $(\cdots)^{*}$ and $(\cdots)^{**}$ denote accordingly some short-lived coupled three-body system.

The twentieth century saw two fundamental revolutions in physics—relativity and quantum theory. If in the theory of relativity time was equated in status to coordinates and Minkowski space was introduced with four-dimensional invariant interval that determines the distance between two events, then in quantum mechanics it remained within the framework of Newton's classical definition [10]. In any case, it can be said that these new concepts did not significantly change the above classical or Newtonian definition of time. In particular, relativistic mechanics only deforms and compresses time without affecting its essence - one-dimensionality, homogeneity and continuity. Unlike the ability of a body to move in opposite directions in space, time is usually considered to have only one dimension and one direction, despite the fact that most laws of physics allow that any process can occur in both forward and backward directions. In modern physics, there are only a small number of known physical phenomena that violate the reversibility of time, which presupposes the presence of a directionality or arrow of time. Let us recall that well-known examples of the arrow of time are [11–17]:

- Time arrow, characteristic of expanding waves (such as light or sound emanating from a source).

- The arrow of time associated with the growth of entropy in an isolated system according to the second law of thermodynamics.
- The arrow of time associated with the irreversibility of measurements in quantum mechanics.
- The arrow of time associated with the preference for a certain direction of time in weak interactions in particle physics (CP symmetry breaking).
- The cosmological arrow of time, which is associated with the expansion of the Universe after the Big Bang.
- An arrow of time that arises from the delay effect associated with the charged particle's electromagnetic radiation reaction, causing it to "remember" the history of its dynamics [18].
- Irreversibility and the arrow of time are characteristic of quantum systems immersed in a fundamental environment, such as a continuously fluctuating quantum vacuum [19,20]. These systems can be called complex or whole system, which is more than the sum of their parts [17].

Note that the fundamentality of the various arrows of time and their interrelationship is a hotly debated topic in modern theoretical physics (see, for example, [21]).

Our main goal is to study the issue of irreversibility in classical mechanics and the role of time, or more precisely, the parameter of chronologization of the motion stages of a classical dynamical system. To do this, we consider the general classical three-body problem, which is quite well studied and in a certain sense is a reference example of a dynamical system.

Recall that the study of the three-body problem for celestial mechanics is still in demand, both from the point of view of finding new periodic trajectories [22,23] and in studying the dynamics of supermassive stellar systems that curve space, which automatically makes interaction three-particle [24].

It should also be noted that this problem plays an important role in the context of quantum-classical matching during the transition of a complex dynamical system from the region of quantum motion to the region of classical chaotic motion (Poincaré systems). In addition, the study of this problem is of great practical importance since a significant amount of the scientific and technical information about atomic-molecular processes known and used by us can be described within the framework of the three-body model (see, for example, [25]).

It is important to recall that geometrization methods for dynamical problems have long been used by many researchers to justify the description of the irreversible and chaotic nature of dynamical systems using statistical methods [4,5,26–31].

A mathematical feature of the three-body problem is that it is generally described by an eighth-order system of stiff differential equations, the stability of which requires calculations with a very small time step. The problem becomes even more complicated when we consider a multichannel scattering problem, taking into account arbitrary, including three-particle interactions, which is typical for all atom-molecular processes. In this case, as a rule, over a wide range of initial data of the problem, the system exhibits chaotic behavior. Note that, due to these difficulties, no reliable solver has yet been created for mass calculations of multichannel atom-molecular processes.

In other words, new studies of the three-body problem are highly relevant both from the point of view of identifying new features of dynamic systems and for creating an effective mathematical tool for numerical modeling of the problem.

To study this question, we recently considered the multichannel scattering in a three-body system (see diagram in Figure 1), formulating it in a conformal Euclidean–Riemannian space associated with the potential energy surface of the system of interacting bodies [5]. The developed representation made it possible to identify two new hidden symmetries of the internal motion of a three-body system and thereby reduce the number of equations of motion to six instead of the usual eight. Note that when moving to a local reference system, a new parameter of the chronologization of the phases of motion of the dynamical

system "s" appears in the problem. This parameter, as we will see below, in the global coordinate system $s \mapsto \mathfrak{s}$ (where $\mathfrak{s}$ is the chronolization parameter in the global coordinate system) actually represents the trajectory of the center of mass of the three-body system in the three-dimensional configuration space, which we will further call *internal time* . It is obvious that the internal time $\mathfrak{s}$ will be multidimensional, non-uniform and oriented, whereas in classical mechanics the time "t" has an absolute value and does not depend on the processes occurring in the system.

All this ultimately leads to a more accurate description of the stages of evolution of an irreversible system, in this case the process of multichannel scattering in a three-body system (see diagram in Figure 1). The article derives an Equation for the density distribution of geodesic trajectories in phase space, on the basis of which the entropy of the trajectory flow is constructed. The new definition of entropy differs from the definition of Kolmogorov-Sinai [32–34] and Pesin [35] entropy as applied to dynamical systems and allows one to strictelly construct a measure of the complexity of a low-dimensional dynamical system. A new definition of the dimension of the fractal structure of the internal time of the restricted three-body problem, different from the Hausdorff-Besicovitch criterion, was also investigated and given. As numerous numerical experiments show, the internal time $\mathfrak{s}$ immersed in three-dimensional space always has a dimension less than one and is equal to 0.89.

The article is organized as follows:

In Section 1, we briefly introduce the role of time and, in general, the chronologizing parameter for the description of dynamic systems, in particular, using the example of a three-body classical system in classical mechanics.

In Section 2, we present the problem statement and derive differential equations describing the motion of three bodies in a local coordinate system, as well as an underdetermined system of algebraic equations that allows us to construct transformations between local and global coordinate systems in differential form. An integral representation for the three-dimensional internal time of a three-particle dynamical system in global coordinates Jacobi is constructed.

In Section 3, we present mathematical algorithms for organizing simulation of the problem on high-performance computing machines. A mathematical algorithm for calculating three-dimensional manifolds is described in detail, using which two complete members of different families of manifolds are calculated and visualized. A mathematical algorithm has been created for solving the trajectory problem in a local coordinate system, the potentials of pair interactions between particles have been specified, and the initial conditions for solving Cauchy problem have been formulated.

In Section 4, we analyze in detail the mechanisms of occurrence of randomness in the geodesic trajectories of a deterministic dynamical system and formulate a criterion for the divergence of two close geodesic trajectories, similar to the Lyapunov exponent. A system of stochastic differential Equations is determined, with the help of which an second-order partial differentialEquation is obtained that describes the evolution of the distribution of conditional probability in the flow of geodesic trajectories.

In Section 5, we define the nonstationary probability distribution and the normal probability distribution in a geodesic trajectory flow. By analogy with Shannon's entropy, we define the entropy of a low-dimensional dynamical system and its measure of complexity. A formula is obtained to calculate the region of classical chaos in phase space. An analogue of the Lyapunov exponential for the wave function of a quantum three-body system has been determined.

In Section 6, the properties of the internal time of a restricted three-particle problem on manifolds $\mathcal{A}_1$ and $\mathcal{B}_1$, respectively, are investigated using numerical simulation. The divergence of close internal times on the specified manifolds is investigated, and the corresponding Lyapunov exponents are calculated. This section also provides numerical calculations of the dimension of fractal internal times from their length.

In Section 7, we discuss the obtained theoretical and numerical results and outline directions for future research.

2. Formulation of the Problem

In the 20th century, physics experienced a qualitative transition from the simplicity of reductionism to the complexity of chaos theory, which ultimately fundamentally changed our understanding of complex phenomena, ushering in the development of a new discipline—complexity science. Note that pioneering work on chaos theory was carried out by H. Poincaré when studying the three-body problem of celestial mechanics [36]. He showed that even simple deterministic systems can exhibit aperiodic, chaotic behavior that is very sensitive to initial conditions, which in turn challenged Laplace's philosophical view of a deterministic universe [37].

In the present work, we consider a more general formulation of the three-body problem, namely, multichannel scattering (see diagram in Figure 1) with arbitrary interactions potential between bodies, including taking into account three-particle interactions. In particular, the solution of the problem requires 18 (6 × 3) first integrals of motion. In general, as E. Bruns [38] showed (see also the book [39]), the n-body problem with $n \geq 3$, taking into account the binary interaction between particles, admits only 10 first integrals and is thus not integrable. It should be noted that although the three-body problem is non-integrable, in some special cases, it is possible to calculate analytical solutions, the so-called *homographic solutions* (see for example [40]). Nevertheless, it is worth noting a clear example from classical mechanics that demonstrates the chaotic behavior of a system even in the case of four coupled first-order ordinary differential equations derived from Hamilton's equations of motion.

As recently shown in [5], a representation developed on the basis of the formulation of the three-body problem on a conformally Euclidean space associated with the potential energy surface of the system of bodies allows one to discover new hidden internal symmetries of the dynamical system. Note that this makes it possible to carry out a more complete integration in the general case of the non-integrable three-body problem and reduce it to a 6th order system instead of the usual 8th order. In the local reference frame $\{\bar{x}\} = (x^1, x^2, x^3) \in \mathcal{M}_t^{(3)}$, the dynamical system is described by the following set of first-order stiff *ordinary differential equations* (ODEs):

$$\begin{cases} \dot{\zeta}^1 = a_1\{(\zeta^1)^2 - (\zeta^2)^2 - (\zeta^3)^2 - \Lambda^2\} + 2\zeta^1\{a_2\zeta^2 + a_3\zeta^3\}, & \zeta^1 = \dot{x}^1, \\ \dot{\zeta}^2 = a_2\{(\zeta^2)^2 - (\zeta^3)^2 - (\zeta^1)^2 - \Lambda^2\} + 2\zeta^2\{a_3\zeta^3 + a_1\zeta^1\}, & \zeta^2 = \dot{x}^2, \\ \dot{\zeta}^3 = a_3\{(\zeta^3)^2 - (\zeta^1)^2 - (\zeta^2)^2 - \Lambda^2\} + 2\zeta^3\{a_1\zeta^1 + a_2\zeta^2\}, & \zeta^3 = \dot{x}^3, \end{cases} \quad (1)$$

where $\mathcal{M}_t^{(3)}$ is a bundle of the three-dimensional manifold $\mathcal{M}^{(3)}$, which is defined by the metric tensor $g_{ij}(\{\bar{x}\}) = g(\{\bar{x}\})\delta_{ij},\ i,j = 1,2,3$. In the system of Equation (1) $\dot{\zeta}^i = d\zeta^i/ds$ denotes the derivative with respect to the chronolizing parameter "s", which is determined using the sum of integrals in the local coordinate system $\{\bar{x}\}$:

$$s(\{\bar{x}\}) = \sum_{i=1}^{3} \int \sqrt{g(\{\bar{x}\})} dx^i. \quad (2)$$

In addition, the following notations are made:

$$a_i(\{\bar{x}\}) = -\frac{\partial \ln \sqrt{g(\{\bar{x}\})}}{\partial x^i}, \quad \Lambda(\{\bar{x}\}) = \frac{J}{g(\{\bar{x}\})}, \quad g(\{\bar{x}\}) = \frac{[E - U(\{\bar{x}\})]}{U_0} > 0. \quad (3)$$

where $J = const$ denotes the total angular momentum of three-body system, $E = const$ and $U(\{\bar{x}\})$ are the total energy and potential energy of the system of bodies, respectively, $U_0 = \max U(\{\bar{x}\}) = const$, and δ_{ij} is the Kronecker delta.

It is easy to check that the system of Equation (1) is invariant under the change $s \to -s$, i.e., is reversible with respect to the chronolizing parameter or the *internal time* in the local reference frame $s(\{\bar{x}\})$. Note that $s(\{\bar{x}\})$ being a function of local coordinates and during the evolution of a dynamical system represents a continuous and one-dimensional curve, which in all features is equivalent to the definition of the usual time, i.e., $s(\{\bar{x}\}) \equiv t$.

For a comprehensive and detailed study of the properties of the *internal time* $\mathfrak{s}(\{\bar{\rho}\})$, we need to move to the global or Jacobian coordinate system $\{\bar{\rho}\} = (\rho_1, \rho_2, \rho_3) \in \mathbb{R}^3$, where $\mathbb{R}^3$ is a three-dimensional Euclidean space (see Figure 2). Recall that only in this system, one can reproduce the explicit form of the metric tensor element $g(\{\bar{x}\}) = \overline{g}(\{\bar{\rho}\})$ and get the opportunity to study the structure and the nature of the chronological parameter $\mathfrak{s}(\{\bar{\rho}\})$.

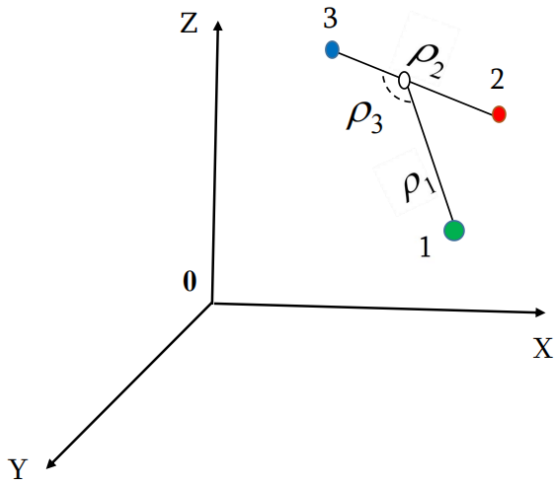

Figure 2. In the Cartesian coordinate system (X, Y, Z), the Jacobi coordinates $\{\bar{\rho}\} = (\rho_1, \rho_2, \rho_3)$ are shown, where the colored circles indicate bodies 1, 2 and 3, and the colorless circle respectively indicates the center of mass of bodies 2 and 3.

A completely different picture emerges when considering the chronologizing parameter in the global coordinate system $\mathfrak{s}(\{\bar{\rho}\})$. During the evolution of the dynamical system, this parameter, as a continuous curve, will fill the space $\mathbb{R}^3$, in some sense similar to the three-dimensional Hilbert curve [41]. Moreover, its two-dimensional projections can have non-trivial topological features characterized by Betti number [42], and metric properties will be described by invariant measures and fractal dimensions [43]. In what follows, the chronologizing parameter in the global system $\mathfrak{s}(\{\bar{\rho}\})$, which is diametrically different from the usual time "t", will be called the *internal time* of the three-body dynamical system.

As shown, transformations between local $\{\bar{x}\}$ and global $\{\bar{\rho}\}$ coordinate systems can be represented only in differential form [5]:

$$\begin{cases} d\rho_1 = \alpha_1 dx^1 + \alpha_2 dx^2 + \alpha_3 dx^3, \\ d\rho_2 = \beta_1 dx^1 + \beta_2 dx^2 + \beta_3 dx^3, \\ d\rho_3 = \lambda_1 dx^1 + \lambda_2 dx^2 + \lambda_3 dx^3, \end{cases} \tag{4}$$

where the coefficients $(\alpha_1, \cdots, \beta_1, \cdots, \lambda_3)$ are solutions of an underdetermined system of algebraic equations of the following form:

$$\begin{aligned} &\alpha_1^2 + \beta_1^2 + \lambda_1^2 = \overline{g}(\{\bar{\rho}\}), \qquad &&\alpha_1\alpha_2 + \beta_1\beta_2 + \lambda_1\lambda_2 = 0, \\ &\alpha_2^2 + \beta_2^2 + \lambda_2^2 = \overline{g}(\{\bar{\rho}\}), \qquad &&\alpha_1\alpha_3 + \beta_1\beta_3 + \lambda_1\lambda_3 = 0, \\ &\alpha_3^2 + \beta_3^2 + \lambda_3^2 = \overline{g}(\{\bar{\rho}\}), \qquad &&\alpha_2\alpha_3 + \beta_2\beta_3 + \lambda_2\lambda_3 = 0. \end{aligned} \tag{5}$$

It is not difficult to verify that the system of Equation (5), which consists of 6 Equations and 9 unknowns, can generate three-dimensional oriented smooth manifolds $\mathcal{R}^{(3)}$, which

are immersed in nine-dimensional Euclidean space $\mathbb{R}^9$. The number of such manifolds can be easily calculated using the well-known combinatorial formula $C_n^m = \frac{n!}{m!(n-m)!}$, which determines the number of n-permutations of the set m. Considering that $n = 9$ denotes the number of unknowns, and $m = 6$, respectively, the number of equations, then the generated manifolds will be 84. As the analysis of the symmetry properties of the system of Equations shows (5), only four families of manifolds are possible.

For definiteness, below we will consider the first two families, each of which consists of six manifolds; $\mathcal{A} = (\mathcal{A}_1, \mathcal{A}_2, \mathcal{A}_3, \mathcal{A}_4, \mathcal{A}_5, \mathcal{A}_6)$ and $\mathcal{B} = (\mathcal{B}_1, \mathcal{B}_2, \mathcal{B}_3, \mathcal{B}_4, \mathcal{B}_5, \mathcal{B}_6)$, where each family member is determined by three independent parameters, such as:

$$\mathcal{A} = \big\{(\alpha_1, \alpha_2, \alpha_3), (\beta_1, \beta_2, \beta_3), (\lambda_1, \lambda_2, \lambda_3), (\alpha_1, \beta_1, \lambda_1), (\alpha_2, \beta_2, \lambda_2), (\alpha_3, \beta_3, \lambda_3)\big\},$$

and respectively for the family:

$$\mathcal{B} = \big\{(\alpha_1, \beta_2, \lambda_3), (\alpha_1, \beta_3, \lambda_2), (\alpha_2, \beta_1, \lambda_3), (\alpha_2, \beta_3, \lambda_1), (\alpha_3, \beta_1, \lambda_2), (\alpha_3, \beta_2, \lambda_1)\big\}.$$

Finally, we can combine each family of manifolds as a direct sum of sets:

$$\mathcal{R}_{\mathcal{A}}^{(3)} \cong \bigcup_{i=1}^{6} \mathcal{R}_{\mathcal{A}_i}^{(3)}, \qquad \mathcal{R}_{\mathcal{B}}^{(3)} \cong \bigcup_{i=1}^{6} \mathcal{R}_{\mathcal{B}_i}^{(3)}.$$

In a similar way, we can construct different families of manifolds.

It is important to note that each manifold of a given family is also surrounded by two additional manifolds, the direct products of which form a nine-dimensional manifold. In particular, the manifold $\mathcal{R}_{\mathcal{A}_1}^{(3)} = \mathcal{R}_{(\alpha_1,\alpha_2,\alpha_3)}^{(3)}$ is surrounded by two additional manifolds $\mathcal{R}_{(\beta_1,\lambda_2,\beta_3)}^{(3)}$ and $\mathcal{R}_{(\lambda_1,\beta_2,\lambda_3)}^{(3)}$, which can be combined using the direct product $\mathcal{R}_{\mathcal{A}_1}^{(9)} = \mathcal{R}_{\mathcal{A}_1}^{(3)} \times \mathcal{R}_{(\beta_1,\lambda_2,\beta_3)}^{(3)} \times \mathcal{R}_{(\lambda_1,\beta_2,\lambda_3)}^{(3)}$. Below we will call $\mathcal{R}_{\mathcal{A}_1}^{(9)}$ a complete member of the $\mathcal{A}$ family. As for the complete member of the family $\mathcal{B}$, it can be represented in the form $\mathcal{R}_{\mathcal{B}_1}^{(9)} = \mathcal{R}_{\mathcal{B}_1}^{(3)} \times \mathcal{R}_{(\alpha_2,\beta_3,\lambda_1)}^{(3)} \times \mathcal{R}_{(\alpha_3,\beta_1,\lambda_2)}^{(3)}$, where $\mathcal{R}_{\mathcal{B}_1}^{(3)} = \mathcal{R}_{(\alpha_1,\beta_2,\lambda_3)}^{(3)}$.

Now let us move on to constructing the form of *internal time* in the global coordinate system $\mathfrak{s}(\{\bar{\rho}\})$. Using the inverse transformation, we can express increments in local coordinates in terms of increments in global Jacobi coordinates:

$$\begin{cases} dx^1 = \breve{\alpha}_1 d\rho^1 + \breve{\alpha}_2 d\rho_2 + \breve{\alpha}_3 d\rho_3, \\ dx^2 = \breve{\beta}_1 d\rho^1 + \breve{\beta}_2 d\rho_2 + \breve{\beta}_3 d\rho_3, \\ dx^3 = \breve{\lambda}_1 d\rho^1 + \breve{\lambda}_2 d\rho_2 + \breve{\lambda}_3 d\rho_3, \end{cases} \tag{6}$$

where the coefficients $(\breve{\alpha}_1, \cdots, \breve{\alpha}_3, \cdots, \breve{\lambda}_3)$ are determined by the following formulas:

$$\begin{array}{lll} \breve{\alpha}_1 = (\beta_2\lambda_3 - \beta_3\lambda_2)A, & \breve{\alpha}_2 = (\beta_3\lambda_1 - \beta_1\lambda_3)A, & \breve{\alpha}_3 = (\beta_1\lambda_2 - \beta_2\lambda_1)A, \\ \breve{\beta}_1 = (\alpha_3\lambda_2 - \alpha_2\lambda_3)A, & \breve{\beta}_2 = (\alpha_1\lambda_3 - \alpha_3\lambda_1)A, & \breve{\beta}_3 = (\alpha_2\lambda_1 - \alpha_1\lambda_2)A, \\ \breve{\lambda}_1 = (\alpha_2\beta_3 - \alpha_3\beta_2)A, & \breve{\lambda}_2 = (\alpha_3\beta_1 - \alpha_1\beta_3)A, & \breve{\lambda}_3 = (\alpha_1\beta_2 - \alpha_2\beta_1)A, \end{array} \tag{7}$$

in addition, $A = 1/[\alpha_1\beta_2\lambda_3 + \alpha_2\beta_3\lambda_1 + \alpha_3\beta_1\lambda_2 - \alpha_1\beta_3\lambda_2 - \alpha_2\beta_1\lambda_3 - \alpha_3\beta_2\lambda_1]$ is a determinant. Now, taking into account the Equation (2), for internal time we get the following expression:

$$\mathfrak{s}(\{\bar{\rho}\}) = s_0 + \alpha \int_{\rho_1^0}^{\rho_1} \sqrt{\bar{g}(\{\bar{\rho}\})} d\rho_1 + \beta \int_{\rho_2^0}^{\rho_2} \sqrt{\bar{g}(\{\bar{\rho}\})} d\rho_2 + \lambda \int_{\rho_3^0}^{\rho_3} \sqrt{\bar{g}(\{\bar{\rho}\})} d\rho_3, \tag{8}$$

where the following notations are made; $\alpha = \sum_{i=1}^{3} \breve{\alpha}_i$, $\beta = \sum_{i=1}^{3} \breve{\beta}_i$ and $\lambda = \sum_{i=1}^{3} \breve{\lambda}_i$.

Note that the internal time $\mathfrak{s}(\{\bar{\rho}\})$ in the form of a curve in three-dimensional space appears in the asymptotic subspace (in), then goes into one of the asymptotic subspace (out), while it is wound in a complicated way around of the selected curve $\mathfrak{s}_i$, $i = \overline{1,3}$ connecting two asymptotic subspaces (see Figure 3).

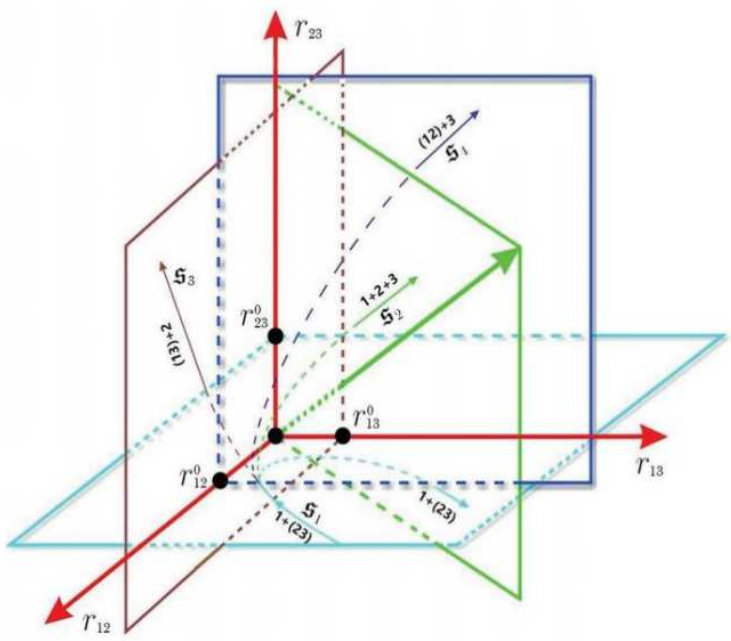

Figure 3. The set of smooth curves $\mathfrak{s} = (\mathfrak{s}_1, \mathfrak{s}_2, \mathfrak{s}_3, \mathfrak{s}_4)$ connecting the asymptotic subspace (in), in which the three-body system $1 + (23)$ is grouped, with other asymptotic subspaces (out), where the particles are grouped as follows: $1 + (23)$, $(12) + 3$, $(13) + 2$, and $1 + 2 + 3$. The distance between particles "i" and "j" in the Cartesian coordinate system is given by the expression $r_{ij}(\{\bar{\rho}\})$ $(i, j = 1, 2, 3,\ i \neq j)$, and r^0_{ij} - the average distance between particles in the corresponding pairs. During the scattering process, the three-dimensional internal time $\mathfrak{s}(\{\bar{\rho}\})$, which has an arrow, selects a specific asymptotic subspace for transition, which in some conditions may be random.

Thus, we have formulated all the necessary mathematical formulas for studying the general three-body problem (see diagram in Figure 1) by calculating the trajectory of the reduced mass of three bodies $\mu_0 = \sqrt{\frac{m_1 m_2 m_3}{m_1+m_2+m_3}}$, where m_1, m_2 and m_3, in three-dimensional configuration space $\mathbb{R}^3$.

3. Mathematical Algorithm for Numerical Simulation of the Three-Body Problem

3.1. Model of Pair Interaction Potentials Between Particles

As we see, the system of ordinary differential Equation (1) can be simulated numerically after specifying the interaction potential between bodies in the global coordinate system. In particular, for the sake of certainty, we will assume that the interaction between two arbitrary pairs of bodies is determined by the Morse potential, which is characteristic of short-range intermolecular forces:

$$U(r_{ij}) = U^{(0)}_{ij}\left[1 - \exp\{-b_{ij}(r_{ij} - r^0_{ij})\}\right]^2, \qquad i, j = 1, 2, 3, \quad i \neq j, \tag{9}$$

where r_{ij} is the distance between particles "i" and "j", the term $U^{(0)}_{ij} = const$ denotes the depth of the interaction potential, $b_{ij} > 0$ is a certain constant specific to a particular pair of interacting particles and r^0_{ij} is the equilibrium communication distance. Recall that the Morse potential is often used in molecular physics because it well describes the interaction of two atoms in a bound state within a diatomic molecule.

Note that these potentials must be written in Jacobi coordinate system, which can be done using the following coordinate transformations:

$$r_{12} = \sqrt{\rho_1^2 + (\mu_- \rho_2)^2 - 2\mu_- \rho_1 \rho_2 \cos\vartheta},$$
$$r_{13} = \sqrt{\rho_1^2 + (\mu_+ \rho_2)^2 + 2\mu_+ \rho_1 \rho_2 \cos\vartheta}, \qquad r_{23} = \rho_2, \tag{10}$$

where $\mu_- = m_3/(m_2 + m_3)$ and $\mu_+ = m_2/(m_2 + m_3)$, in addition, m_2 and m_3 are the particle masses.

To carry out specific calculations it is necessary to determine the full potential of interaction between particles $\overline{g}(\{\bar{\rho}\}) = [E - U_{12}(\{\bar{\rho}\}) - U_{13}(\{\bar{\rho}\}) - U_{23}(\{\bar{\rho}\})]$. Using the data Table 1, it is possible to calculate the energy surface of an elementary process, i.e., construct the metric function $\overline{g}(\{\bar{\rho}\})$ (see Figure 4), which is a necessary condition for the complete formulation of a mathematical problem and its preparation for numerical modeling.

Table 1. Parameters for determining the total interaction potential of a model three-body system.

$U_{12}^{(0)} = U_{13}^{(0)} = U_{23}^{(0)}$	$b_{12} = b_{13} = b_{23}$	$r_{12}^0 = r_{13}^0 = r_{23}^0$	E
1	0.25	2.0	2.5
1	0.25	2.0	3.5

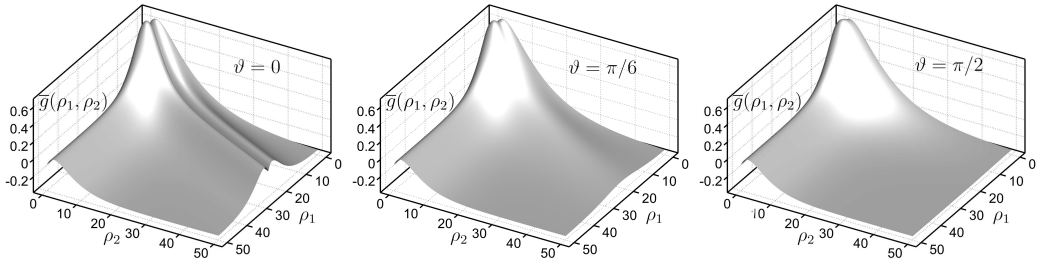

Figure 4. Energy surface of interaction particles for three different scattering angles. Recall that ρ_3 in Jacobi coordinates determines the scattering angle, i.e., $\rho_3 = \vartheta$ (see Figure 2).

Recall that the energy surface plots with data from the second row of Table 1 are not given here, since they are similar to the previous one and only are slightly shifted upward due to the large energy value.

3.2. Underdetermined Algebraic Equations and 3D-Manifolds Generated by Them

As we have seen, a system of underdetermined algebraic Equation (5) plays a key role in transformations between local and global coordinate systems. It is convenient to study this system by writing it in a dimensionless form, in which all the geometric and topological properties of the manifolds generated by it are preserved:

$$\begin{aligned} \bar{\alpha}_1^2 + \bar{\beta}_1^2 + \bar{\lambda}_1^2 &= 1, & \bar{\alpha}_1\bar{\alpha}_2 + \bar{\beta}_1\bar{\beta}_2 + \bar{\lambda}_1\bar{\lambda}_2 &= 0, \\ \bar{\alpha}_2^2 + \bar{\beta}_2^2 + \bar{\lambda}_2^2 &= 1, & \bar{\alpha}_1\bar{\alpha}_3 + \bar{\beta}_1\bar{\beta}_3 + \bar{\lambda}_1\bar{\lambda}_3 &= 0, \\ \bar{\alpha}_3^2 + \bar{\beta}_3^2 + \bar{\lambda}_3^2 &= 1, & \bar{\alpha}_2\bar{\alpha}_3 + \bar{\beta}_2\bar{\beta}_3 + \bar{\lambda}_2\bar{\lambda}_3 &= 0, \end{aligned} \tag{11}$$

where $\bar{\alpha}_i = \bar{\alpha}_i/g(\{\bar{x}\})$, $\bar{\beta}_i = \bar{\beta}_i/g(\{\bar{x}\})$ and $\bar{\lambda}_i = \bar{\lambda}_i/g(\{\bar{x}\})$, where $i = 1, 2, 3$.

First, the values for the selected triple of parameters are set. By arbitrarily setting their values from the interval $(-1, +1)$, we can determine the values of the remaining six parameters. Solutions to each triple of parameters generate three-dimensional manifolds, the number of which, as indicated above, is equal to 84. Note that we do not consider possible complex solutions to system (11). Depending on the initial triples of parameters specified, the methods for finding the values of the remaining parameters differ significantly from each other. Let us briefly consider the case of specifying $(\bar{\alpha}_1, \bar{\alpha}_2, \bar{\alpha}_3)$, which requires

an iterative approach. Note that the calculation algorithm itself belongs to the family of gradient methods—the method of conjugate directions.

After a random selection of parameter values $(\bar{\alpha}_1, \bar{\alpha}_2, \bar{\alpha}_3)$, the system of Equation (11) is completely determined, i.e., becomes an algebraic system of six Equations with six unknowns $(\bar{\beta}_1, \bar{\beta}_2, \bar{\beta}_3; \bar{\lambda}_1, \bar{\lambda}_2, \bar{\lambda}_3)$ that can be solved exactly. In particular, from the Equation (11) one can obtain:

$$\begin{aligned}
g_1 &= \bar{\beta}_1^2 + \bar{\lambda}_1^2 - (1 - \bar{\alpha}_1^2) = \bar{\beta}_1^2 + \bar{\lambda}_1^2 - C_1, & C_1 &= 1 - \bar{\alpha}_1^2,\\
g_2 &= \bar{\beta}_2^2 + \bar{\lambda}_2^2 - (1 - \bar{\alpha}_2^2) = \bar{\beta}_2^2 + \bar{\lambda}_2^2 - C_2, & C_2 &= 1 - \bar{\alpha}_2^2,\\
g_3 &= \bar{\beta}_3^2 + \bar{\lambda}_3^2 - (1 - \bar{\alpha}_3^2) = \bar{\beta}_3^2 + \bar{\lambda}_3^2 - C_3, & C_3 &= 1 - \bar{\alpha}_3^2,\\
g_4 &= \bar{\alpha}_1\bar{\alpha}_2 + \bar{\beta}_1\bar{\beta}_2 + \bar{\lambda}_1\bar{\lambda}_2 = \bar{\beta}_1\bar{\beta}_2 + \bar{\lambda}_1\bar{\lambda}_2 + C_4, & C_4 &= \bar{\alpha}_1\bar{\alpha}_2,\\
g_5 &= \bar{\alpha}_1\bar{\alpha}_3 + \bar{\beta}_1\bar{\beta}_3 + \bar{\lambda}_1\bar{\lambda}_3 = \bar{\beta}_1\bar{\beta}_3 + \bar{\lambda}_1\bar{\lambda}_3 + C_5, & C_5 &= \bar{\alpha}_1\bar{\alpha}_3,\\
g_6 &= \bar{\alpha}_2\bar{\alpha}_3 + \bar{\beta}_2\bar{\beta}_3 + \bar{\lambda}_2\bar{\lambda}_3 = \bar{\beta}_2\bar{\beta}_3 + \bar{\lambda}_2\bar{\lambda}_3 + C_6, & C_6 &= \bar{\alpha}_2\bar{\alpha}_3.
\end{aligned} \tag{12}$$

For further research, we introduce new notations:

$$\mathbf{g} = \begin{pmatrix} g_1 \\ g_2 \\ \vdots \\ g_6 \end{pmatrix}, \qquad \mathbf{x} = \begin{pmatrix} \bar{\beta}_1 \\ \bar{\beta}_2 \\ \vdots \\ \bar{\lambda}_3 \end{pmatrix}.$$

We set the objective function $K(\mathbf{x})$:

$$K(\mathbf{x}) = \sum_{i=1}^{6} [g_i(\mathbf{x})]^2 = (\mathbf{g} \cdot \mathbf{g}). \tag{13}$$

Let us define the gradient of the function $K(\mathbf{x})$:

$$\nabla K(\mathbf{x}) = \begin{pmatrix} \frac{\partial K}{\partial x_1} \\ \\ \frac{\partial K}{\partial x_2} \\ \vdots \\ \frac{\partial K}{\partial x_6} \end{pmatrix} = 2 \begin{pmatrix} 2g_1\bar{\beta}_1 + g_4\bar{\beta}_2 + g_5\bar{\beta}_3 \\ 2g_2\bar{\beta}_2 + g_4\bar{\beta}_1 + g_6\bar{\beta}_3 \\ 2g_3\bar{\beta}_3 + g_5\bar{\beta}_1 + g_6\bar{\beta}_2 \\ 2g_1\bar{\lambda}_1 + g_4\bar{\lambda}_2 + g_5\bar{\lambda}_3 \\ 2g_2\bar{\lambda}_2 + g_4\bar{\lambda}_1 + g_6\bar{\lambda}_3 \\ 2g_3\bar{\lambda}_3 + g_5\bar{\lambda}_1 + g_6\bar{\lambda}_2 \end{pmatrix} = 2W'K(\mathbf{x}),$$

where W' is the transposed Jacobian matrix W:

$$W = \begin{pmatrix} 2\bar{\beta}_1 & 0 & 0 & 2\bar{\lambda}_1 & 0 & 0 \\ 0 & 2\bar{\beta}_2 & 0 & 0 & 2\bar{\lambda}_2 & 0 \\ 0 & 0 & 2\bar{\beta}_3 & 0 & 0 & 2\bar{\lambda}_3 \\ \bar{\beta}_2 & \bar{\beta}_1 & 0 & \bar{\lambda}_2 & \bar{\lambda}_1 & 0 \\ \bar{\beta}_3 & 0 & \bar{\beta}_1 & \bar{\lambda}_3 & 0 & \bar{\lambda}_1 \\ 0 & \bar{\beta}_3 & \bar{\beta}_2 & 0 & \bar{\lambda}_3 & \bar{\lambda}_2 \end{pmatrix}, \qquad W' = \begin{pmatrix} 2\bar{\beta}_1 & 0 & 0 & \bar{\beta}_2 & \bar{\beta}_3 & 0 \\ 0 & 2\bar{\beta}_2 & 0 & \bar{\beta}_1 & 0 & \bar{\beta}_3 \\ 0 & 0 & 2\bar{\beta}_3 & 0 & \bar{\beta}_1 & \bar{\beta}_2 \\ 2\bar{\lambda}_1 & 0 & 0 & \bar{\lambda}_2 & \bar{\lambda}_3 & 0 \\ 0 & 2\bar{\lambda}_2 & 0 & \bar{\lambda}_1 & 0 & \bar{\lambda}_3 \\ 0 & 0 & 2\bar{\lambda}_3 & 0 & \bar{\lambda}_1 & \bar{\lambda}_2 \end{pmatrix}.$$

In iterative methods, the main difficulty usually lies in the correct choice of the initial approximation. For the general case, we do not have a clearly defined criterion for setting such initial values. Therefore, we set the initial approximation $\mathbf{x}^{(0)}$ as follows:

$$\mathbf{x}^{(0)} = \begin{pmatrix} \bar{\beta}_1^{(0)} \\ \bar{\beta}_2^{(0)} \\ \vdots \\ \bar{\lambda}_3^{(0)} \end{pmatrix}, \qquad \begin{aligned} \bar{\beta}_1^{(0)} &= \pm\sqrt{(1 - \bar{\alpha}_1^2)/2}, & \bar{\lambda}_1^{(0)} &= \pm\bar{\beta}_1^{(0)},\\ \bar{\beta}_2^{(0)} &= \pm\sqrt{(1 - \bar{\alpha}_2^2)/2}, & \bar{\lambda}_2^{(0)} &= \pm\bar{\beta}_2^{(0)},\\ \bar{\beta}_3^{(0)} &= \pm\sqrt{(1 - \bar{\alpha}_3^2)/2}, & \bar{\lambda}_3^{(0)} &= \pm\bar{\beta}_3^{(0)}. \end{aligned} \tag{14}$$

The signs in the initial approximation $\mathbf{x}^{(0)}$ of system (14) are set randomly, but so that for the first three approximations and the next three values the signs are not the same. This is due to the form of the last three equations of system (12).

Finally, we can set the calculation algorithm:

$$\mathbf{x}^{(n+1)} = \mathbf{x}^{(n)} + \delta_n \mathbf{p}^{(n)}, \quad \mathbf{p}^{(n)} = -\nabla K(\mathbf{x}^{(n)}) + \gamma_{n-1}\mathbf{p}^{(n-1)}, \qquad n = 1, 2, \ldots \tag{15}$$

where $\mathbf{p}^{(n)}$ is the direction of descent, δ_n is the step of descent and the coefficient γ_n, which is defined below in step 4.

1. We set the initial approximation $\mathbf{p}^{(0)}$:

$$\mathbf{p}^{(0)} = -\nabla K(\mathbf{x}^{(0)}), \qquad n = 0,$$

2. Determine the next value $\mathbf{x}^{(1)}$:

$$\mathbf{x}^{(1)} = \mathbf{x}^{(0)} + \delta_0 \mathbf{p}^{(0)}.$$

The value of the descent step δ_n $(n \geqslant 0)$ is searched numerically until the condition is met:

$$K(\mathbf{x}^{(n)} + \delta_n \mathbf{p}^{(n)}) < K(\mathbf{x}^{(n)}), \qquad \nabla K(\mathbf{x}^{(n)}) = 2W'(\mathbf{x}^{(n)})\mathbf{g}(\mathbf{x}^{(n)}).$$

3. We calculate the term $\mathbf{p}^{(1)}$:

$$\mathbf{p}^{(1)} = -\nabla K(\mathbf{x}^{(1)}) + \gamma_0 \mathbf{p}^{(0)}.$$

4. The coefficients γ_{n-1} are calculated using the formula:

$$\gamma_{n-1} = \frac{\left[\left(\nabla K(\mathbf{x}^{(n)}), \nabla K(\mathbf{x}^{(n)})\right) - \nabla K(\mathbf{x}^{(n-1)})\right]}{|\nabla K(\mathbf{x}^{(n-1)})|^2}, \qquad n \geqslant 1,$$

5. For subsequent n we repeat steps 2-4 until the condition $|\nabla K(\mathbf{x}^{(n)})| \leqslant \varepsilon_1$, where ε_1 is the specified accuracy.

After obtaining a chain of approximations $\mathbf{x}^{(n)}$ upon reaching the end condition of iterations 5, we refine the initial initial data $(\bar{\alpha}_1, \bar{\alpha}_2, \bar{\alpha}_3)$. Note that the following notations are used above:

$$|\mathbf{y}|^2 = \sum_{i=1}^{6} y_i^2, \qquad (\mathbf{a}, \mathbf{b}) = \sum a_i b_i.$$

The refined initial approximation is obtained from the correction of the initial data parameters $(\bar{\alpha}_1, \bar{\alpha}_2, \bar{\alpha}_3)$ according to the original scheme (14). This is justified by the fact that initially the value of the triple of parameters is chosen randomly.

Then we carry out the next stage of iterations using the described method 1–5. The end of such an outer iteration occurs when the condition is met; $|\nabla K(\mathbf{x}^{(n)})| \leqslant \varepsilon_2$.

In order to avoid excessive iteration steps or looping, an additional limitation on the number of iterations is introduced. Recall that during the calculations the values were specified $\varepsilon_1 = 10^{-9}$ and $\varepsilon_2 = 10^{-18}$. Such values make it possible to determine the roots of the algebraic system (11) with an accuracy at which $g_i \approx 10^{-10}$, $i = 4, 5, 6$ and $g_i \approx 10^{-16}$, $i = 1, 2, 3$ for the system (12).

The solution of Equations system (11) for the original triplets $(\bar{\beta}_1, \bar{\beta}_2, \bar{\beta}_3)$ and $(\bar{\lambda}_1, \bar{\lambda}_2, \bar{\lambda}_3)$ is similar to the method described above. To illustrate the calculations, we present here two complete members of the families of manifolds $\mathcal{A}$ and $\mathcal{B}$ (see Figures 4 and 5), on which we will further study the dynamics of the classical three-body system.

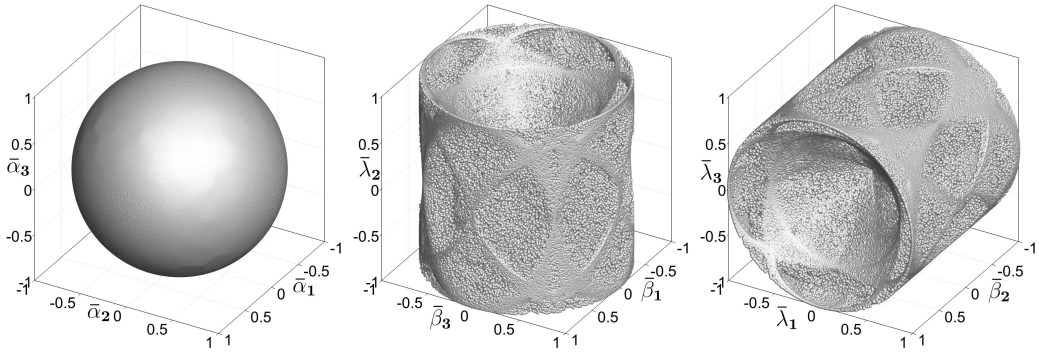

Figure 5. A manifold of the family $\mathcal{A}$, which has the form $\mathcal{R}^{(3)}_{(\beta_1,\lambda_2,\beta_3)}$ (sphere) and two additional manifolds surrounding it from left to right $\mathcal{R}^{(3)}_{(\beta_1,\lambda_2,\beta_3)}$ and $\mathcal{R}^{(3)}_{(\lambda_1,\beta_2,\lambda_3)}$. Combining these manifolds by a direct product, we obtain a complete member of the family $\mathcal{A}$, which can be represented in the following form $\mathcal{R}^{(9)}_{\mathcal{A}_1} = \mathcal{R}^{(3)}_{(\beta_1,\lambda_2,\beta_3)} \times \mathcal{R}^{(3)}_{(\beta_1,\lambda_2,\beta_3)} \times \mathcal{R}^{(3)}_{(\lambda_1,\beta_2,\lambda_3)}$.

3.3. Mathematical Algorithm for Modeling a Trajectory Problem

Let us rewrite the system of differential Equation (1) in a local coordinate system. In general, it can be represented as follows:

$$\frac{d\mathbf{Y}}{dt} = \mathbf{\Phi}(t; u, v, w, x^1, x^2, x^3), \tag{16}$$

where $u = \dot{x}^1$, $v = \dot{x}^2$ and $w = \dot{x}^3$, in addition, the following notations are introduced:

$$\mathbf{Y} = \begin{pmatrix} u \\ v \\ w \\ x^1 \\ x^2 \\ x^3 \end{pmatrix}, \qquad \mathbf{\Phi} = \begin{pmatrix} \Phi_1 \\ \Phi_2 \\ \Phi_3 \\ \Phi_4 \\ \Phi_5 \\ \Phi_6 \end{pmatrix} = \begin{pmatrix} a_1(u^2 - v^2 - w^2 - \Lambda^2) + 2u(a_2 v + a_3 w) \\ a_2(v^2 - w^2 - u^2 - \Lambda^2) + 2v(a_3 w + a_1 u) \\ a_3(w^2 - u^2 - v^2 - \Lambda^2) + 2w(a_1 u + a_2 v) \\ u \\ v \\ w \end{pmatrix}. \tag{17}$$

For the system of differential Equation (16), the Cauchy problem with initial conditions is posed:

$$\mathbf{Y}(t_0) = \mathbf{Y}_0. \tag{18}$$

According to the Runge–Kutta method, the approximate value of $\mathbf{Y_{i+1}}$ is calculated using the formulas with a step Δt:

$$\mathbf{Y}_{i+1} = \mathbf{Y}_i + \Delta\mathbf{Y}_i, \qquad i = 0, 1, 2, \ldots \tag{19}$$

where

$$\Delta\mathbf{Y}_i = \frac{1}{6}\left[\mathbf{k}_1^{(j)} + 2\mathbf{k}_2^{(j)} + 2\mathbf{k}_3^{(j)} + \mathbf{k}_4^{(j)}\right], \qquad j = \overline{1,6}. \tag{20}$$

In addition, the following notations are made in (19):

$$\begin{aligned}
\mathbf{k}_1^{(j)} &= \Delta t \cdot \mathbf{\Phi}^j(t_i, u_i, v_i, w_i, x_i^1, x_i^2, x_i^3), \\
\mathbf{k}_2^{(j)} &= \Delta t \cdot \mathbf{\Phi}^j\left[t_i + \frac{\Delta t}{2}, u_i + \frac{\mathbf{k}_1^{(1)}}{2}, v_i + \frac{\mathbf{k}_1^{(2)}}{2}, w_i + \frac{\mathbf{k}_1^{(3)}}{2}, x_i^1 + \frac{\mathbf{k}_1^{(4)}}{2}, x_i^2 + \frac{\mathbf{k}_1^{(5)}}{2}, x_i^3 + \frac{\mathbf{k}_1^{(6)}}{2}\right], \\
\mathbf{k}_3^{(j)} &= \Delta t \cdot \mathbf{\Phi}^j\left[t_i + \frac{\Delta t}{2}, u_i + \frac{\mathbf{k}_2^{(1)}}{2}, v_i + \frac{\mathbf{k}_2^{(2)}}{2}, w_i + \frac{\mathbf{k}_2^{(3)}}{2}, x_i^1 + \frac{\mathbf{k}_2^{(4)}}{2}, x_i^2 + \frac{\mathbf{k}_2^{(5)}}{2}, x_i^3 + \frac{\mathbf{k}_2^{(6)}}{2}\right], \\
\mathbf{k}_4^{(j)} &= \Delta t \cdot \mathbf{\Phi}^j\left[t_i + \Delta t, u_i + \mathbf{k}_3^{(1)}, v_i + \mathbf{k}_3^{(2)}, w_i + \mathbf{k}_3^{(3)}, x_i^1 + \mathbf{k}_3^{(4)}, x_i^2 + \mathbf{k}_3^{(5)}, x_i^3 + \mathbf{k}_3^{(6)}\right].
\end{aligned} \tag{21}$$

Note that during calculations the calculation step remains constant, equal to $\Delta t = 10^{-4}$.

Solving the system of Equations (16) and (17) we obtain the trajectory of the center of mass of the three-body system in the local coordinate system. For the final presentation of the results, they must be presented in the system of Jacobi variables (global variables). Using differential representations for global coordinates (4), we can write the following expressions:

$$\begin{aligned}
\rho_1 &= \rho_{01} + \int_{x_0^1}^{x^1} \alpha_1 dx + \int_{x_0^2}^{x^2} \alpha_2 dy + \int_{x_0^3}^{x^3} \alpha_3 dz = \rho_{01} + \alpha_1 \Delta x^1 + \alpha_2 \Delta x^2 + \alpha_3 \Delta x^3, \\
\rho_2 &= \rho_{02} + \int_{x_0^1}^{x^1} \beta_1 dx + \int_{x_0^2}^{x^2} \beta_2 dy + \int_{x_0^3}^{x^3} \beta_3 dz = \rho_{02} + \beta_1 \Delta x^1 + \beta_2 \Delta x^2 + \beta_3 \Delta x^3, \\
\rho_3 &= \rho_{03} + \int_{x_0^1}^{x^1} \lambda_1 dx + \int_{x_0^2}^{x^2} \lambda_2 dy + \int_{x_0^3}^{x^3} \lambda_3 dz = \rho_{03} + \lambda_1 \Delta x^1 + \lambda_2 \Delta x^2 + \lambda_3 \Delta x^3,
\end{aligned} \tag{22}$$

where $\Delta x^1 = x^1 - x_0^1$, $\Delta x^2 = x^2 - x_0^2$ and $\Delta x^3 = x^3 - x_0^3$, in addition, $\{\bar{x}_0\} = (x_0^1, x_0^2, x_0^3)$ and $\{\bar{\rho}_0\} = (\rho_{01}, \rho_{02}, \rho_{03})$ denote the initial coordinate values in the local and global coordinate systems, respectively.

In the same way, we can define equations for velocities in global coordinate system using increments of velocities in local coordinates:

$$\begin{cases}
\dot{\rho}_1 = \dot{\rho}_{01} + \alpha_1 \Delta u + \alpha_2 \Delta v + \alpha_3 \Delta w, \\
\dot{\rho}_2 = \dot{\rho}_{02} + \beta_1 \Delta u + \beta_2 \Delta v + \beta_3 \Delta w, \\
\dot{\rho}_3 = \dot{\rho}_{03} + \lambda_1 \Delta u + \lambda_2 \Delta v + \lambda_3 \Delta w,
\end{cases}$$

where $\dot{\rho}_{01}$, $\dot{\rho}_{02}$ and $\dot{\rho}_{03}$ denote the components of the initial velocity of the center of mass of a three-body system in global coordinates.

The initial value of the coordinate of the phase point in the local system $\{\bar{x}_0\} = (x_0^1, x_0^2, x_3^3)$ at moment $s = 0$ must correspond to the initial value $\{\bar{\rho}_0\} = (\rho_{01}, \rho_{02}, \rho_{03})$ at moment $t = 0$. Due to the specifics of calculating such evolutionary problems, the initial values $\{\bar{x}\}$ and $\{\dot{\bar{x}}\}$ can be taken as the values of the coordinates and velocity of the point of the previous step of the system calculation at the moment $t = t_0 + \Delta t$, where Δt is the time step for the local coordinate system, t_0 is the origin of the count at this step.

For definiteness, we will assume that the three bodies have the same masses and at the moment $t = 0$ form an equilateral triangle in the Cartesian coordinate system. In this case, the initial values of the Jacobi coordinates will be as follows:

$$\rho_1|_{t=0} = \rho_{01} = \frac{\sqrt{3}}{2}, \qquad \rho_2|_{t=0} = \rho_{02} = 1, \qquad \rho_3|_{t=0} = \rho_{03} = \frac{\pi}{2}. \tag{23}$$

It is very important now to synchronize the initial coordinate values in the Jacobi system $\{\bar{\rho}\} \in \mathbb{R}^{(3)}$ and in the local coordinate system $\{\bar{x}\} \in \mathcal{R}_{\mathcal{F}}^{(3)}$, where $\mathcal{F} = (\mathcal{A}_1; \mathcal{B}_1)$ describes two families of manifolds. Using Equations (6) and (7), we can write the following transformations for the position and velocity of the reduced mass μ_0 in the local coordinate system:

$$\begin{aligned}
x^1|_{t=0} &= x_0^1 = \breve{\alpha}_1 \rho_{01} + \breve{\alpha}_2 \rho_{02} + \breve{\alpha}_3 \rho_{03}, & \dot{x}^1|_{t=0} &= \dot{u}_0 = \breve{\alpha}_1 \dot{\rho}_{01} + \breve{\alpha}_2 \dot{\rho}_{02} + \breve{\alpha}_3 \dot{\rho}_{03}, \\
x^2|_{t=0} &= x_0^2 = \breve{\beta}_1 \rho_{01} + \breve{\beta}_2 \rho_{02} + \breve{\beta}_3 \rho_{03}, & \dot{x}^2|_{t=0} &= \dot{v}_0 = \breve{\beta}_1 \dot{\rho}_{01} + \breve{\beta}_2 \dot{\rho}_{02} + \breve{\beta}_3 \dot{\rho}_{03}, \\
x^3|_{t=0} &= x_0^3 = \breve{\lambda}_1 \rho_{01} + \breve{\lambda}_2 \rho_{02} + \breve{\lambda}_3 \rho_{03}, & \dot{x}^3|_{t=0} &= \dot{w}_0 = \breve{\lambda}_1 \dot{\rho}_{01} + \breve{\lambda}_2 \dot{\rho}_{02} + \breve{\lambda}_3 \dot{\rho}_{03}.
\end{aligned} \tag{24}$$

Thus, now we have all the tools to organize the numerical integration of the trajectory problem in the global Jacobi coordinate system.

4. Geodesic Trajectories Flow in the Phase Space

4.1. Lyapunov Exponent for Geodesic Trajectories Flow

As the analysis shows, a multichannel process (see Figure 1) in a three-body system is not only irreversible in the general case, but can also exhibit random behavior during its evolution. To study the nature of motion in a three-particle dynamical system, one can, like the Lyapunov exponent [44], introduce a parameter showing the degree of divergence of close geodesic trajectories. In particular, the average growth rate of the distance between neighboring trajectories of the center of mass of bodies system is determined by the leading Lyapunov exponent, which for a long (but not too long) time t can be estimated as:

$$\epsilon(t) \simeq \frac{1}{t} \cdot \ln \left\| \frac{\Delta\mathfrak{s}(t)}{\Delta\mathfrak{s}(0)} \right\|, \tag{25}$$

where $s \equiv t$ is one-dimensional and homogeneous time, and $\Delta\mathfrak{s}(t) = \mathfrak{s}(t) - \mathfrak{s}'(t)$ denotes the difference of two close internal times or geodetic trajectories, in addition, $\Delta\mathfrak{s}(0) \ll 1$ is the distance between two trajectories at the initial moment $t = 0$. In what follows, $\epsilon(t)$ will be called the leading time-dependent Lyapunov exponent. Note that the time-dependent Lyapunov exponent, as we will see below, will play a key role in studying the properties of the geodesic trajectories flow in phase space.

Definition 1. *Let us call the standard leading Lyapunov exponent the parameter characterizing the asymptotic behavior of the sequence* $\left\| \frac{\Delta\mathfrak{s}(t)}{\Delta\mathfrak{s}(0)} \right\|$*:*

$$\epsilon := \overline{\lim_{t\to\infty}} \left[\frac{1}{t} \cdot \ln \left\| \frac{\Delta\mathfrak{s}(t)}{\Delta\mathfrak{s}(0)} \right\| \right], \qquad t \neq 0, \tag{26}$$

where $a := b$ *means that* a *is assumed to be equal to* b *and the constant* $\epsilon = const$*, which can be either positive or negative and equal to* 0*.*

4.2. Equation of Motion of Geodesic Trajectories Flow in Phase Space

Since the system of Equations (1) is rigid and, moreover, nonlinear, it is very difficult to expect that to solve it it will always be possible to create a more or less reliable mathematical algorithm that will ensure the stability of numerical calculations. In the case when the time-dependent Lyapunov exponent is positive, that is $\epsilon(t) > 0$ (see (25)), the system experiences chaotic motion, so it makes sense not to study the problem of single geodesic trajectories, but to consider the evolution of the flow of geodesic trajectories on the corresponding three-dimensional manifolds.

In other words, it makes sense to consider a trajectory problem with a random external influence, which for the three-body problem can be written as a system of stochastic differential Equations of the Langevin type (see also Equations of motion in conformal Euclidean space (1)):

$$\dot{z}^\mu = A^\mu(\{\bar{x}\}, \{\dot{\bar{x}}\}) + f^\mu(t), \qquad \mu = \overline{1,6}, \tag{27}$$

where the following notations are made for the independent variables:

$$\{z\} = \left(z^1 = \dot{x}^1; \quad z^2 = \dot{x}^2; \quad z^3 = \dot{x}^3; \quad z^4 = x^1; \quad z^5 = x^2; \quad z^6 = x^3\right)$$

and for the terms $A^\mu(\{\bar{x}\}, \{\dot{\bar{x}}\})$ included in the Equation (27), respectively, the following notations:

$$\begin{cases} A^1 = a_1\{(\dot{x}^1)^2 - (\dot{x}^2)^2 - (\dot{x}^3)^2 - \Lambda^2\} + 2\dot{x}^1\{a_2\dot{x}^2 + a_3\dot{x}^3\}, & A^4 = x^1, \\ A^2 = a_2\{(\dot{x}^2)^2 - (\dot{x}^3)^2 - (\dot{x}^1)^2 - \Lambda^2\} + 2\dot{x}^2\{a_3\dot{x}^3 + a_1\dot{x}^1\}, & A^5 = x^2, \\ A^3 = a_3\{(\dot{x}^3)^2 - (\dot{x}^1)^2 - (\dot{x}^2)^2 - \Lambda^2\} + 2\dot{x}^3\{a_1\dot{x}^1 + a_2\dot{x}^2\}, & A^6 = x^3. \end{cases} \tag{28}$$

For definiteness, below we will use a random Gauss-Markovian process as the forces $f^{\mu}(t)$:

$$\langle f^{\mu}(t)\rangle = 0, \qquad \langle f^{\mu}(t) f^{\mu}(t')\rangle = \epsilon(t)\,\delta(t-t'), \tag{29}$$

where $\epsilon(t) > 0$ is the degree of the random process, which in the problem under consideration is a time-dependent Lyapunov exponent (see Equation (25)).

Thus, in the deterministic three-body problem, randomities have been identified that arise due to the influence of the nonlinearity of the Equations (1)) and the underdetermination of the system of algebraic Equations (5), providing transitions between the local and global coordinate systems. To carry out analytical studies, we assumed that the emerging randomness $f^{\mu}(t)$ obeys the Gauss-Markovian process and are generated from a single source. Recall that this approach is in some sense equivalent to the statistical approach implemented in [29], where the exact but unknown evolution of the scalar curvature is replaced by a statistical approximation.

To exclude the occurrence of other unnatural random influences on the dynamical system, the Equations (27)–(29) must be defined in a local coordinate system along regular curves on the manifolds $\mathcal{R}^{(9)}_{\mathcal{A}_1}$ and $\mathcal{R}^{(9)}_{\mathcal{B}_1}$, respectively.

Theorem 1. *If we assume that geodesic trajectories in phase space are described by the Equations (27) and (28), and random forces satisfy the correlation conditions (29), then the geodesic flow in phase space will satisfy the following Fokker-Planck type equation:*

$$\frac{\partial \mathcal{P}}{\partial t} = \sum_{\mu=1}^{6}\left\{\epsilon(t)\frac{\partial^2}{\partial z_{\mu}^2} + \frac{\partial}{\partial z_{\mu}} A^{\mu}(\{z\})\right\}\mathcal{P}. \tag{30}$$

Proof. Let us consider the following functional that describes the evolution of the conditional probability distribution of a geodesic flow in phase space:

$$\mathcal{P}(\{z\},t;\{z'\},t') = \left\langle \prod_{\mu=1}^{6} \delta[z^{\mu}(t) - z^{\mu}(t')]\right\rangle. \tag{31}$$

Differentiating expression (31) with respect to the usual time "t", taking into account Equations (27) and (28), we obtain:

$$\partial_t \mathcal{P}(\{z\},t;\{z'\},t') = -\sum_{\nu=1}^{6}\partial_{z^{\nu}}\left\langle z_t^{\nu}\prod_{\mu=1}^{6}\delta[z^{\mu}(t)-z^{\mu}(t')]\right\rangle =$$

$$\sum_{\nu=1}^{6}\partial_{z^{\nu}}\Big\{\mathbf{A}(\{z\},\{\dot{z}\})\mathcal{P}(\{z\},t;\{z'\},t') + \langle f(t)\delta[z^{\mu}(t)-z^{\mu}(t')]\Big\}, \tag{32}$$

where

$$\mathbf{A}(\{z\},\{\dot{z}\}) = \begin{cases} A^1(\{z\},\{\dot{z}\}), \\ \quad . \quad . \quad . \quad , \\ A^6(\{z\},\{\dot{z}\}). \end{cases} \tag{33}$$

Taking into account that the random process $f(t)$ satisfies the correlation relations (29), we can calculate the second term in expression (32). In particular, using Wick's theorem for an arbitrary functional $N(\{z\},f(t))$, one can obtain:

$$\langle f(t)N(\{z\},t;\{z'\},t')\rangle = 2\left\langle\frac{\delta N}{\delta f(t)}\right\rangle = 2\frac{\partial}{\partial z^{\mu}}\left\langle\frac{\delta z^{\mu}(t)}{\delta f(t)}\delta(z^{\mu}(t)-z^{\mu}(t')\right\rangle. \tag{34}$$

Recall that $\{z\} = (z^1, \cdots, z^6)$ denotes a set of stochastic functions whose variational derivatives with respect to the independent random force $f(t)$ are defined as follows:

$$\left\langle \frac{\delta z^{\mu}(t)}{\delta f(t)} \right\rangle = \epsilon(t) \cdot \mathrm{sgn}(t - t') + O(t - t'). \tag{35}$$

After carrying out the regularization procedure in the sense of the Fourier expansion, we find its value at the time:

$$t = t' : \mathrm{sgn}(0) = \frac{1}{2}. \tag{36}$$

Taking into account the Equalities in (32)–(36) for the conditional probability, we obtain the Fokker–Planck Equation of the form (30).

Note that the equation for the evolution of the probability density of the flow of geodesic trajectories (30) in phase space is given in local coordinates $\{\bar{x}\}$, in which the chronolization parameter "t" varies as ordinary, one-dimensional and homogeneous time along the numerical axis from the past to the future through the present. Using coordinate transformations (4), one can specify the interaction potential between particles in global Jacobi coordinates $\{\bar{\rho}\}$ and calculate the evolution of the flow of geodesic trajectories in the phase space in local coordinates, including when a dynamical system passes from one asymptotic subspace to another. Finally, we note that using direct (4) and inverse (6) coordinate transformations, one can calculate the evolution of the probability density distribution in global, Jacobi coordinates, i.e., find $\check{\mathcal{P}}(\{\bar{\rho}\}, \{\dot{\bar{\rho}}\}, t)$. □

5. Entropy of the Flow of Geodesic Trajectories and Complexity Criterion

Shannon entropy is an effective dynamical indicator that provides a direct measure of the rate of diffusion of geodesic flow, hence the time scale of instabilities encountered when dealing with chaos. Note that this allows us to more reliably explain the nature of a nonlinear dynamical system characterized by complexity and nonequilibrium.

Definition 2. *Let us call the probability density of the geodesic flow in phase space the expression:*

$$\mathcal{P}^0(\{z\}, t) = \mathcal{P}(\{z\}, t; \{z'\}, t')\big|_{\{z'\}=0,\, t'=0'} \tag{37}$$

which is normalized to unity.

Definition 3. *Let us call the equilibrium probability distribution of geodesic flow in phase space the expression:*

$$\bar{\mathcal{P}}^0(\{z\}, t) = \mathcal{P}(\{z\}, t; \{z'\}, t')\big|_{[\epsilon=\epsilon_0,\, \{z'\}=0,\, t'=0]'} \tag{38}$$

where $\epsilon_0 = \int_0^T \epsilon(t)dt/T$*, in addition,* T *denotes some finite time interval.*

By analogy with Shannon entropy [45], which characterizes the average rate of information creation by a stochastic data source, for a continuous flow of geodesic trajectories of a low-dimensional dynamical system, entropy can be introduced in the form:

$$\mathcal{S}(t) = -\int_{\mathbb{R}^6} \mathcal{P}^0(\{z\}, t) \ln \mathcal{P}^0(\{z\}, t) dz^1 \cdots dz^6, \tag{39}$$

where $\mathbb{R}^6 \ni \overline{z^1, z^6}$ denotes the phase space.

The Three-Body Problem as a Low-Dimensional System with Complexity

The complexity of systems is usually associated with the difficulty of understanding and describing them. However, after Kolmogorov formulated the concept of computational complexity [46], it became clear that the complexity of a system could be associated with information [47]. Subsequently, complexity also became associated with open systems and with the unpredictable behavior of highly nonlinear systems [48,49]. Recently a new

meaning has emerged regarding systems theory [50], which states that complexity is half the way to "equilibrium" and "disequilibrium" [51]. As we noted above, in a three-particle system, under certain conditions, non-integrability and chaos can arise. In this case, it is convenient to describe the dynamical system in phase space using probabilistic methods (see (30)).

Since a three-particle dynamical system under certain conditions can have probabilistic properties, then for it, by analogy with a statistical ensemble, a criterion or measure of complexity can be introduced:

$$\mathcal{C}(t) = \mathcal{S}(t)\mathcal{K}(t), \tag{40}$$

where $\mathcal{S}(t)$ is "information", which is defined by the Equation (39) and a shift from the quilibrium probability distribution (38) or "disequilibrium" $\mathcal{K}(t)$, which is defined as follows:

$$\mathcal{K}^{1/2}(t) = \left| \int_{\mathbb{R}^6} \Delta\mathcal{P}^0(\{z\},t) dz^1 \cdots dz^6 \right|, \tag{41}$$

where $\Delta\mathcal{P}^0(\{z\},t) = \mathcal{P}^0(\{z\},t) - \bar{\mathcal{P}}^0(\{z\},t)$.

Fundamentally important information about the behavior of the quantum three-body problem can be obtained by integrating the probability distribution of the geodesic flow over phase space:

$$I^0(t) = \int_{\mathbb{R}^6} \check{\mathcal{P}}^0(\{z\},t) dz^1 \cdots dz^6, \tag{42}$$

where $\check{\mathcal{P}}^0(\{z\},t)$ is the probability distribution normalized to unity at the initial time $t = 0$.

Recall that the integral (42) determines the average volume of the phase space subject to classical chaos. In the case, when the classical region of chaos in the phase space exceeds the size of the quantum cell $\hbar^n$ (where $2n$ is the dimension of the phase space), which in this case is equivalent to the inequality $I^0(t) > \hbar^3$, then quantum averaging does not eliminate chaos in the quantum system (see [52]). Moreover, in this case, the main object of quantum mechanics—the wave function of the system—becomes chaotic. It is obvious that in this case the quantization of the classical dynamical system must be carried out differently from the standard approach [5].

In this case, for low-dimensional quantum chaotic systems, a criterion similar to the Lyapunov exponent can be determined. In particular, for finite time intervals this exponent can be determined by the following formula:

$$\epsilon_q(t) \simeq \frac{1}{t} \cdot \ln \left\| \frac{\overline{\delta\Psi(\mathfrak{s})}}{\overline{\delta\Psi(0)}} \right\|, \qquad \overline{\delta\Psi}(\mathfrak{s}) = \int_{\mathcal{M}^{(3)}} \Delta\Psi(\mathfrak{s}) dz^4 dz^5 dz^6, \quad t \neq 0, \tag{43}$$

while in the limit of large times the exponent will tend to a finite limit:

$$\epsilon_q := \overline{\lim_{t\to\infty}} \left[\frac{1}{t} \cdot \ln \left\| \frac{\overline{\delta\Psi(\mathfrak{s})}}{\overline{\delta\Psi(0)}} \right\| \right], \qquad t \neq 0, \tag{44}$$

where $\Psi(\mathfrak{s}, \{\bar{z}\})$ is the wave function of a three-body system, and $\Delta\Psi(\mathfrak{s}) = [\Psi(\mathfrak{s}, \{\bar{z}\}) - \Psi(\mathfrak{s}', \{\bar{z}\})]$ denotes the difference between two wave functions that were close at the initial time $\mathfrak{s} = 0$ and $\{\bar{z}\} = (z^4, z^5, z^6)$.

6. Calculation of the Internal Time of the Restricted Three-Body Problem and Discussions

If we use the data from the first rows of Tables 1 and 2, and also consider the initial configuration of the three bodies given in (23), then, obviously, the system of bodies will be in a bound state throughout the entire time of movement since the binding energy will be greater than the kinetic energy at finite distances (restricted three-body problem). In particular, by calculating the internal time of a dynamical system on complete members of the families of manifolds $\mathcal{A}_1$ and $\mathcal{B}_1$ (see Figures 5 and 6) using the algorithm given in Section 5, we find their three-dimensional images (see Figure 7).

Table 2. For the initial velocities $\{\dot{\rho}\}$ and the moment of inertia of the three-body system J we use the following values.

$\dot{\rho}_1\|_{t=0} = \dot{\rho}_{01}$	$\dot{\rho}_2\|_{t=0} = \dot{\rho}_{02}$	$\dot{\rho}_3\|_{t=0} = \dot{\rho}_{03}$	J
0.01	0.01	0.10	0.30
0.30	0.50	0.40	0.60
1.00	0.80	0.60	0.80

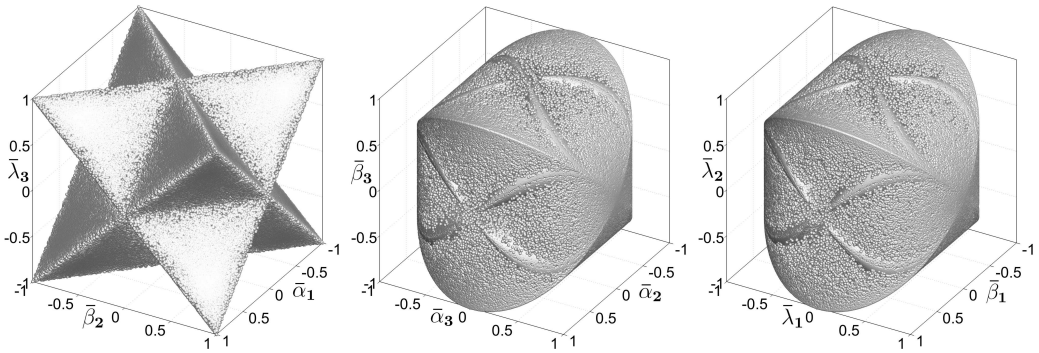

Figure 6. A manifold of the family $\mathcal{B}$, which has the form $\mathcal{R}^{(3)}_{(\alpha_1,\beta_2,\lambda_3)}$ (two three-dimensional pyramids fastened together) and two additional manifolds surrounding it from left to right $\mathcal{R}^{(3)}_{(\alpha_2,\alpha_3,\beta_3)}$ and $\mathcal{R}^{(3)}_{(\beta_1,\lambda_1,\lambda_2)}$. Combining these manifolds by a direct product, we obtain a complete member of the family $\mathcal{B}$, which can be represented in the following form $\mathcal{R}^{(9)}_{\mathcal{B}_1} = \mathcal{R}^{(3)}_{(\alpha_1,\beta_2,\lambda_3)} \times \mathcal{R}^{(3)}_{(\alpha_2,\beta_3,\lambda_1)} \times \mathcal{R}^{(3)}_{(\alpha_3,\beta_1,\lambda_2)}$.

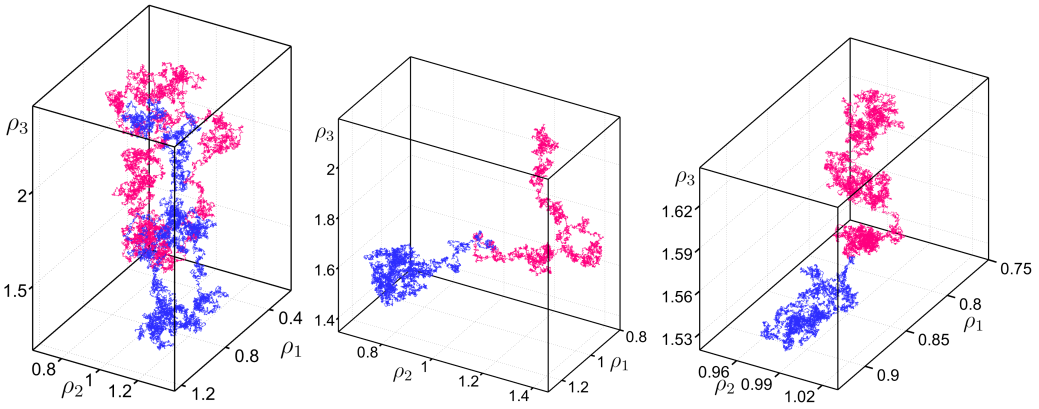

Figure 7. Internal time of three particles for three different initial data on two different complete terms of the manifolds $\mathcal{A}_1$ and $\mathcal{B}_1$. On the plots, blue and red colors indicate internal times that were calculated on the manifolds $\mathcal{A}_1$ and $\mathcal{B}_1$, respectively. Each point of internal time, if projected onto the coordinate axes, determines the configuration of three particles at a given moment.

Analysis of the calculations shows that when using the above initial data, the resulting trajectories indeed describe a restricted three-body problem, however, their nature is chaotic. To make sure that the system's motion is truly chaotic, Lyapunov exponents are calculated for two trajectories whose initial data are close and differ by 10^{-2}. Recall that geodesic trajectories are calculated both on the manifold $\mathcal{A}_1$ and on $\mathcal{B}_1$, see Figures 8 and 9.

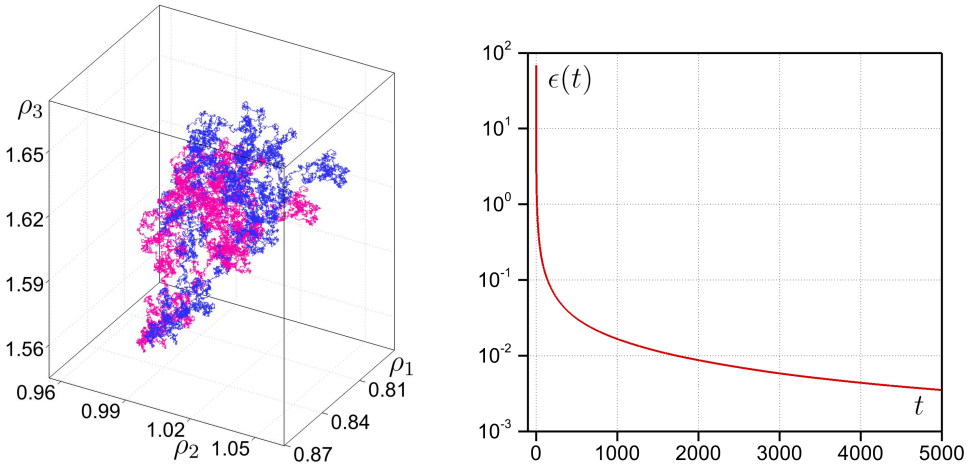

Figure 8. On the left are plots of two internal times $\mathfrak{s}_1(\{\bar{\rho}\})$-(red curve) and $\mathfrak{s}_2(\{\bar{\rho}\})$-(blue curve), which were obtained by calculating on the $\mathcal{A}_1$ manifold with initial conditions differing by 10^{-2}. On the right is a plot of the Lyapunov exponent versus time. As can be clearly seen from the plot, the Lyapunov exponent very slowly tends to zero.

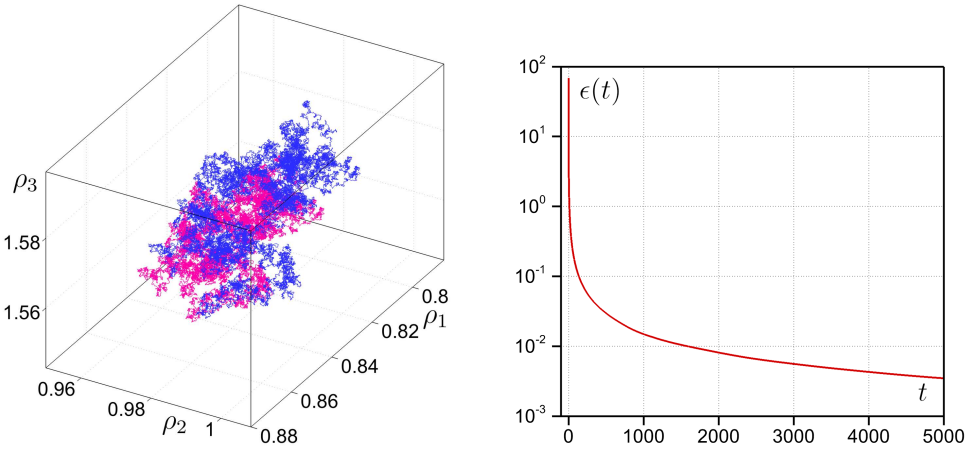

Figure 9. On the left are plots of two internal times $\mathfrak{s}_1(\{\bar{\rho}\})$-(red curve) and $\mathfrak{s}_2(\{\bar{\rho}\})$-(blue curve), which were obtained by calculating on the $\mathcal{B}_1$ manifold with initial conditions differing by 10^{-2}. On the right is a plot of the Lyapunov exponent versus time.

Note that as the usual calculation time "t" increases, the internal time $\mathfrak{s}(\{\bar{\rho}\})$ in all considered cases fills the global three-dimensional space like the three-dimensional Hilbert curve [41], but with the only difference that now the filling occurs chaotically and inhomogeneously.

It is known, the Lyapunov exponent is an important indicator of the behavior of a dynamical system. In particular, when it is positive, i.e., $\epsilon(t) > 0$, then we can talk about the chaotic behavior of the system of particles. As calculations on both manifolds show (see Figures 8 and 9), the Lyapunov exponent is positive. Moreover, for both cases under consideration, depending on the usual time "t", both Lyapunov exponents very slowly tend to zero. Note that such a fairly stable behavior of the Lyapunov exponent is very important for deriving Equations for the probabilistic distribution of the flow of geodesic trajectories in phase space (30). The latter, in turn, makes it possible to construct the entropy of a low-dimensional dynamical system (39), estimate the measure of its complexity (40) and, finally, estimate the degree of its "disequilibrium" (41).

Important characteristics of the internal time of a restricted three-body problem are its macroscopic and microscopic structures in three-dimensional space.

As calculations show, the internal time for the selected initial data continuously fills a certain restricted three-dimensional region, which most likely indicates a certain degree

of ergodicity of the dynamical system. In any case, to be sure of the ergodicity of a low-dimensional dynamical system, it is necessary to carry out additional detailed calculations and studies. It is very possible that for the system under consideration there will be areas of initial data where the ergodicity of the system will be partially or completely violated, for example, in the case of detection of periodic trajectories. However, all this is the subject of new, more detailed research.

Now let us move on to the question, namely: does the random curve have a characteristic feature on large scales?

In particular, as can be seen from the plots in Figures 8 and 9, internal time at different scales is rather random self-similar three-dimensional curves, similar to stochastic fractals, which are known to be non-deterministic [53]. In this regard, a natural question arises: is there any universal characteristic of the three-dimensional random structure formed by internal time?

As well-know, the Hausdorff–Besicovitch exponent is used to determine the dimension of algebraic or geometric fractals, and therefore we cannot use it to calculate the dimension of structures such as a three-dimensional random curve, which is internal time [54]. Recall that random fractals use stochastic rules; for example, Lévy flight, self-avoidance walks, Brownian motion trajectories and Brownian tree, etc. The structure we are studying is close to the concept of the trajectory of Brownian motion, which is a random fractal. Taking this into account, we propose a new criterion for determining the dimension of a stochastic three-dimensional fractal structure.

Definition 4. *Let us call the dimension of a stochastic three-dimensional fractal structure the following expression:*

$$D(t) = \ln\left\{\frac{1}{t}\left|\int_0^t \mathfrak{s}(t')dt'\right|\right\}\Big/\ln t. \tag{45}$$

Using the data from the third row of Table 2, we calculated the internal time on the families of manifolds $\mathcal{A}_1$ and $\mathcal{B}_1$ (see Figure 10). As can be seen from the second figure, internal time as a function of ordinary time is a monotonic function in both cases considered, however, as numerical calculations show, non-monotonic dependencies are also possible, in the case of other initial data. In the third figure on the left, the dimension of fractal structures filling the three-dimensional space of two internal times is calculated. It is shown that the dimension of both structures tends to its limiting asymptotic value $D = 0.89$ at $t \geq 5 \cdot 10^3$.

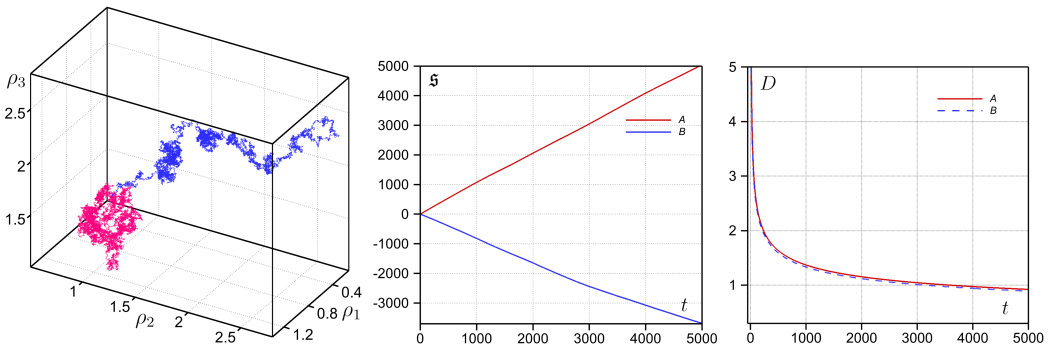

Figure 10. On the left in the first figure, internal times $\mathfrak{s}_1(\{\bar{\rho}\})$-(red curve) and $\mathfrak{s}_2(\{\bar{\rho}\})$-(blue curve) are shown that were calculated on the manifolds' families $\mathcal{A}_1$ and $\mathcal{B}_1$ for the same initial data using the third line of Table 2. The second plot from the left shows the internal time $\mathfrak{s}(t)$ depending the ordinary time "t" for the two marked families of manifolds. As can be seen from the graph, internal time can be either positive or negative. The third figure from the left shows the dimensionality of the structures formed by internal times in three-dimensional space.

In the end, we note that, as preliminary calculations show, the asymptotic value of the dimension of internal time' structures in a number of areas of the initial data of the problem can change and even significantly. We will not touch on these problems, since they require more detailed study.

7. Conclusions

We recently consideried the general three-body problem, which, on the one hand, is quite well studied in classical mechanics and mathematics, and on the other hand, is a referance example of a low-dimensional dynamical system with complexity, a number of aspects of which still remain unexplored [5]. Recall that the problem was formulated in conformal Euclidean space, which is associated with the potential energy of the system of bodies and reflects all its features. This formulation of a deterministic problem allows us to identify new hidden symmetries of the internal motion of a dynamical system and reduce its description in the general case to a sixth-order system instead of an eighth-order one (1), even in the case where the interaction potential is three-particle.

It is shown that a new parameter for chronologizing events of a dynamical system—internal time $\mathfrak{s}(\{\bar{\rho}\})$, which represents the trajectory of the effective mass of a system of bodies μ_0, in contrast to the usual time "t" has a number of unusual properties. In particular, as calculations show, for the restricted three-body problem, the parameter $\mathfrak{s}(\{\bar{\rho}\})$ is in the general case irreversible, multidimensional, inhomogeneous and oriented (has an arrow), which allows the system to choose the preferred asymptotic scattering subspace during the evolution process (see diagram in Figures 1 and 3). In other words, a classical dynamical system consisting of three or more bodies always has a hidden, so-called internal time $\mathfrak{s}(\{\bar{\rho}\}) \mapsto \mathfrak{s}(t)$, which formally has all the above properties.

The work examines in detail the mechanism of the occurrence of randomness in the geodesic trajectory problem of a deterministic system. Recall that the transition to a global reference system is due to the need to perform calculations, which is provided by an underdetermined system of nonlinear algebraic Equation (5). Within the framework of the representation of internal time, a Lyapunov exponent $\epsilon(t)$ (see (25)) dependent on ordinary time is obtained, which determines the rate of divergence of close geodesic trajectories in the flow. Assuming that the randomness in the system has a Gauss-Markovian character with the fluctuation power $\epsilon(t)$, stochastic differential Equations of Langevin type are written for the motion of the representing point with effective mass μ_0. Using these SDEs, a second-order partial differential Equation is obtained that describes the evolution of the probability density of the flow of geodesic trajectories in phase space.

An important achievement of the work is that if we use the representation of internal time to construct the corresponding quantum problem, then we can, without violating the well-known Arnold-Berry theorem [52] in the limit $\hbar \to 0$, move from the region of quantum motion to the region of classical chaotic Poincaré motion, and thereby rigorously solve the problem of quantum-classical matching. In other words, it is precisely this formulation that in certain cases can lead to chaos in the behavior of the wave function of a deterministic quantum system. Let us recall that the criterion for the emergence of quantum chaos is the inequality $I^0(t) > \hbar^3$, where $I^0(t)$ is the volume of the classical chaos region in the phase space.

To verify and test the developed representation using numerical methods, a case was considered in which the interaction between bodies was described using short-range Morse potentials, which is typical for molecular systems. For definiteness, we carried out calculations on two complete members of the families of manifolds $\mathcal{A}_1$ and $\mathcal{B}_1$.

Based on the fact that under certain initial conditions a restricted three-body problem arises, we conducted a detailed study of the properties and structure of three-dimensional internal time, which describes, on the other hand, the trajectory of the effective mass μ_0 in global space $\{\bar{\rho}\} \in \mathbb{R}^3$. As numerical experiments have shown, even in this particular case, internal time $\mathfrak{s}(t)$, in depending of usual time "t" fills three-dimensional space chaotically and inhomogeneously. The work studies in detail the issue of the dimension of stochastic

fractals generated by a dynamical system and defines a new criterion for it (see Definition 4). As shown, for large times $t \geq 5 \cdot 10^3$ the dimension of three-dimensional structures formed by internal time in the case of both manifolds is approximately equal $D = 0.89$.

We expect that the study of the scattering problem in a three-body system within the framework of a new representation [5] will reveal new interesting features of internal time $\mathfrak{s}(t)$, in particular, it will clearly demonstrate the actions of the arrow of internal time when choosing a specific type of elementary atomic-molecular reaction or a certain scattering subspace (see Figure 1).

In conclusion, we note that the developed approach, together with the created algorithm, for the first time provides real opportunities to numerically study a multichannel atomic-molecular process with a given accuracy within the framework of classical mechanics, taking into account the difficulties inherent in integrating stiff systems of ordinary differential equations. The new approach to the geometrization of a dynamical system allows all studies to be carried out not only qualitatively, but also quantitatively in the multidimensional space of the observer, which is extremely important for solving real problems. The approach and the ideas developed in it can be easily generalized to the many-body problem.

And finally, the developed approach may be interesting for studying the dynamics of three massive stellar formations that strongly bend the surrounding space. It is obvious that in such a restricted three-body problem there can be no binary interactions between the bodies and, accordingly, the usual approaches of celestial mechanics must be unacceptable.

Author Contributions: Conceptualization, methodology and investigation, A.S.G.; Funding acquisition and development of mathematical algorithm A.V.B.; Development of mathematical algorithm, simulation and visualization V.V.M. All authors have read and agreed to the published version of the manuscript.

Funding: Gevorkyan A.S. is grateful to grant N 21T-1B059 of the Science Committee of Armenia, which partially funded this work. Bogdanov A.V. acknowledge Saint-Petersburg State University for a research project 95438429.

Data Availability Statement: The data presented in this study are the model data. No new data were created or analyzed in this study. Data sharing is not applicable to this article.

Acknowledgments: A.S.G. thanks L.A. Beklaryan for numerous discussions of the issues raised in this article.

Conflicts of Interest: The author declares no conflict of interest.

References

1. Gowers, T.; Barrow-Green, J.; Leader, I. (Eds.) *The Princeton Companion to Mathematics*; Princeton University Press: Princeton, NJ, USA, 2008.
2. Goody, R.; Goody, R.M.; Goody, R.E. *Principles of Atmospheric Physics and Chemistry*; Oxford University Press: Oxford, UK, 1995; 324p.
3. Briggs, G.A.D.; Butterfield, J.N.; Zeilinger, A. The Oxford Questions on the foundations of quantum physics. *Proc. R. Soc. A* **2013**, *469*, 20130299. [CrossRef] [PubMed]
4. Gevorkyan, A.S. The Three-body Problem in Riemannian Geometry. Hidden Irreversibility of the Classical Dynamical System. *Lob. J. Math.* **2019**, *40*, 1058–1068. [CrossRef]
5. Gevorkyan, A.S. New Concept for Studying the Classical and Quantum Three-Body Problem: Fundamental Irreversibility and Time's Arrow of Dynamical Systems. *Particles* **2020**, *3*, 576–620. [CrossRef]
6. Oxford University Press. The indefinite continued progress of existence and events in the past, present, and future regarded as a whole. In *Oxford Dictionaries: Time;* Oxford University Press: Oxford, UK, 2011.
7. Time. In *The American Heritage Dictionary of the English Language,* 4th ed.; A Nonspatial Continuum in Which Events Occur in Apparently Irreversible Succession from the Past Through the Present to the Future; Houghton Mifflin Harcourt: Boston, MA, USA, 2011.
8. *International Encyclopedy of Phylosopy;* Routledge: Abingdon-on-Thames, UK, 2010.
9. Prigogine, I.; Stengers, I. *Order Out of Chaos: Man's New Dialogue with Nature;* Anglo-America's Preeminent Radical Press—Harper's: New York, NY, USA, 2018.
10. Newton, I. *Mathematical Principles of Natural Philosophy;* Krylov, A.N., Translator; Nauka: Moscow, Russia, 1989.

11. Donoghue, J.F.; Menezes, G. Quantum causality and the arrows of time and thermodynamics. *Prog. Part. Nucl. Phys.* **2020**, *115*, 103812. [CrossRef]
12. Harrington, J. *Time: A Philosophical Introduction;* Bloomsbury Academic: London, UK, 2015; p. 304, ISBN 1472506472.
13. O'Byrne, J.; Kafri, Y.; Tailleur, J.; van Wijland, F. Time irreversibility in active matter, from micro to macro. *Nat. Rev. Phys.* **2022**, *4*, 167–183. [CrossRef]
14. Zeh, H.D. The Nature and Origin of Time-asymmetric Spacetime Structures. In *Springer Handbook of Spacetime Physics;* Ashtekar, A., Petkov, V., Eds.; Springer: Berlin/Heidelberg, Germany, 2014; pp. 185–196. [CrossRef]
15. Hemmo, M.; Shenker, O. The Arrow of Time. In *Cosmological and Psychological Time;* Boston Studies in the Philosophy and History of Science; Dolev, Y., Roubach, M., Eds.; Springer: Cham, Switzerland, 2016; p. 285. [CrossRef]
16. Wuppuluri, S.; Ghirardi, G. (Eds.) *Space, Time and the Limits of Human Understanding;* Springer: Berlin/Heidelberg, Germany, 2017; ISBN 978-3-319-44418-5. [CrossRef]
17. Lineweaver, C.H.; Davies, P.C.W.; Ruse, M. (Eds.) *Complexity and the Arrow of Time;* Cambridge University Press: Cambridge, UK, 2013; p. 357. [CrossRef]
18. Cremaschini, C.; Tessarotto, M. Hamiltonian structure of classical N-body systems of fnite-size particles subject to EM interactions. *Eur. Phys. J. Plus* **2012**, *127*, 4. [CrossRef]
19. Gevorkyan, A.S. Nonrelativistic Quantum Mechanics with Fundamental Environment. *Found. Phys.* **2011**, *41*, 509–515. [CrossRef]
20. Gevorkyan, A.S.; Bogdanov, A.V. Quantum Chromodynamics of the Nucleon in Terms of Complex Probabilistic Processes. *Symmetry* **2024**, *16*, 256. [CrossRef]
21. Coveney, P.; Highfield, R. The Arrow of Time: A Voyage Through Science to Solve Time's Greatest Mystery. In *Science & Society*; Guilford Press: New York, NY, USA, 1991; p. 377.
22. Dmitrašinović, V.; Šuvakov, M.; Hudomal, A. Gravitational Waves from Periodic Three-Body Systems. *Phys. Rev. Lett.* **2014**, *114*, 101102. [CrossRef]
23. Li, X.; Jing, Y.; Lia, S. Over a thousand new periodic orbits of a planar three-body system with unequal masses. *PASJ* **2018**, *70*, 64. [CrossRef]
24. Stone, N.C.; Leigh, N.W.S. A statistical solution to the chaotic, non-hierarchical three-body problem. *Nature* **2019**, *576*, 406–410. [CrossRef]
25. Mirahmadi, M.; Pérez-Ríos, J. Three-body recombination in physical chemistry. *Int. Rev. in Phys. Chem.* **2023**, *41*, 233–267. [CrossRef]
26. Kryulov, N.S. *Foundations of Statistical Physics;* Princeton University Press: Princeton, NJ, USA; Guildford, UK, 1980; p. 283.
27. Gurzadian, V.G.; Savvidy, G.K. Collective Relaxation of Stellar Systems. *Astron. Astrophys.* **1986**, *160*, 203–210.
28. Pettini, M. *Geometry and Topology in Hamiltonian Dynamics and Statistical Mechanics;* Springer: New York, NY, USA, 2007; p. 453.
29. Cassetti, L.; Pettini, M.; Cohen, M.E.G.D. Geometric approach to Hamiltonian dynamics and statistical mechanics. *Phys. Rep.* **2000**, *337*, 237–341. [CrossRef]
30. Eckhardt, B.; Louw, J.A.; Steeb, W.-H. Is there a Connection between Local and Global (In-)Stability? *Aust. J. Phys.* **1986**, *39*, 331–338. [CrossRef]
31. Horwitz, L.; Zion, Y.B.; Lewkowicz, M.; Schiffer, M.; Levitan, J. Geometry of Hamiltonian chaos. *Phys. Rev. Lett.* **2007**, *98*, 234301. [CrossRef] [PubMed]
32. Kolmogorov, A.N. Entropy per unit time as a metric invariant of automorphism. *Dokl. Russ. Acad. Sci.* **1959**, *124*, 754–755.
33. Sinai, Y.G. On the Notion of Entropy of a Dynamical System. *Dokl. Russ. Acad. Sci.* **1959**, *124*, 768–771.
34. Cornfeld, I.P.; Fomin, S.F.; Sinai, Y.G. *Ergodic Theory;* Springer: Berlin/Heidelberg, Germany, 1981.
35. Pesin, Y. Characteristic Lyapunov exponents and smooth ergodic theory. *Russ. Math. Surv.* **1977**, *32*, 55–114. [CrossRef]
36. Poincare, H. *New Methods of Celestial Mechanics;* American Institute of Physics: Woodbury, NY, USA, 1993; Volume 1, Chapter 1.
37. Laplace, P.S. *A Philosophical Essay on Probabilities,* 6th ed.; Truscott, F.W., Emory, F.L., Translators; Dover Publications: New York, NY, USA, 1951.
38. Bruns, E.H. Über die Integrale des Vielekörperproblems. *Acta Math.* **1887**, *11*, 25. [CrossRef]
39. Whittaker, E.T. *A Treatise on the Analytical Dynamics of Particles and Rigid Bodies;* Cambridge University Press: Cambridge, UK, 1989; 456p.
40. Frauenfelder, U.; van Koert, O. *The Restricted Three-Body Problem and Holomorphic Curves;* Springer: Cham, Switzerland, 2018; p. 374. [CrossRef]
41. Hilbert, D. Über die stetige Abbildung einer Linie auf ein Flächenstück. *Math. Ann.* **1891**, *38*, 459–460. [CrossRef]
42. Spanier, E.H. *Algebraic Topology;* Springer: Berlin/Heidelberg, Germany, 1966; ISBN 0-387-94426-5.
43. Badii, R.; Politi, *A. Complexity: Hierarchical Structures and Scaling in Physics;* Cambridge University Press: Cambridge, UK, 1997.
44. Benettin, G.; Galgani, L.; Giorgilli, A.; Strelcyn, J.M. Lyapunov Characteristic Exponents for smooth dynamical systems and for hamiltonian systems; A method for computing all of them. Part 2: Numerical application. *Meccanica* **1980**, *15*, 21–30. [CrossRef]
45. Shannon, C.E. A Mathematical Theory of Communication. *Bell Syst. Tech. J.* **1948**, *27*, 379–423. [CrossRef]
46. Kolmogorov, A.N. Three approaches to the definition of the concept "quantity of information". *Probl. Peredachi Inform.* **1965**, *1*, 3–11.
47. Haken, H. *Information and Self-Organization: A Macroscopic Approach to Complex Systems;* Springer Series in Synergetics; Springer: Berlin/Heidelberg, Germany, 2000.

48. Morin, E. *On Complexity;* Hampton Press: New York, NY, USA, 2008.
49. Nicolis, G.; Prigogine, I. *Self-Organization in Nonequilibrium Systems;* John Wiley and Sons: Hoboken, NJ, USA, 1977.
50. Von Bertalanffy, L. *General System Theory: Foundations, Development, Applications;* George Braziller Inc.: New York, NY, USA, 1968.
51. Kaneko, K.; Tsuda, I. *Complex Systems: Chaos and Beyond;* Springer: Berlin, Germany, 2001.
52. Schuster, H.G. *Deterministic Chaos: An Introduction;* Wiley: Hoboken, NJ, USA, 1984.
53. Rahman, R.; Nowrin, F.; Rahman, M.S.; Wattis, J.A.; Hassan, M.K. Stochastic fractal and Noether's theorem. *Phys. Rev. E* **2021**, *103*, 022106. [CrossRef]
54. Falconer, K.J. *Fractal Geometry. Mathematical Foundations and Applications;* John Wiley and Sons, Inc.: Hoboken, NJ, USA, 2003.